Worsnop *et al. Fire Ecology* (2026) 22:51
https://doi.org/10.1186/s42408-026-00492-6

Fire Ecology

Association for Fire Ecology

RESEARCH

Open Access

# Characterizing windows of opportunity for prescribed pile and broadcast burning in Northern California

Rochelle P. Worsnop[1*], Andrew Hoell[1], Benjamin J. Hatchett[2,3], Teresa B. Chapman[4], Melissa L. Breeden[1], Zach Tolby[5], Karen C. Short[6] and Mike Hobbins[1,7]

## Abstract

**Background** To make strategic decisions about safety and resource allocation, managers must understand when prescribed burn windows of opportunity occur, how they vary throughout the year, and how to anticipate them. For two burn types—pile and broadcast—we characterize the temporal and spatial distributions of past "go-burn" days identified from a database of 15,468 burn permits from 2011 to 2024 in the Northern California Geographic Area Coordination Center's region. We assess the mean temporal evolution of daily anomalies of local- and synoptic-scale environmental variables that occurred in the 2 weeks surrounding those ignitions. We then estimate the mean number of historical burn windows for both burn types in each month using a novel approach to define our prescription criteria. This approach defines the criteria based on ranges of environmental conditions present on past go-burn days.

**Results** Broadcast burns exhibit a strong seasonal signal with the greatest number of ignitions in June and October. Pile burns were four times more numerous than broadcast burns and occurred most often in November–December. Ignition locations varied by month and burn type; e.g., piles ignited in the fall most often occurred in the Sierra while piles ignited in the spring most often occurred in the Foothills ecoregion. Composite local- and synoptic-scale variables indicated preferences for certain environmental conditions depending on the month. Conditions preceding February broadcast burns exhibited warming and drying near the surface and anomalous ridge patterns in the upper atmosphere. Pile burns in October were associated with cooler and wetter surface conditions and anomalous trough patterns aloft. The expected number of burn windows varied by month and burn type (e.g., broadcast burn windows were, on average, three times more likely than those of piles in October).

**Conclusions** We found that ample opportunities exist in northern California for burning throughout the year, yet those opportunities heavily depend on burn type. Findings herein are useful for determining favorable environmental patterns that create burn windows and for identifying priority locations and times to implement broadcast and pile burns.

**Keywords** Broadcast burning, Burn permit data, Burn windows of opportunity, Fire weather, Northern California, Pile burning, Prescribed burning, Synoptic-scale weather, Wildfire mitigation tools

*Correspondence:
Rochelle P. Worsnop
rochelle.worsnop@noaa.gov
Full list of author information is available at the end of the article

**Resumen**

**Antecedentes** Para tomar decisiones estratégicas sobre seguridad y ubicación de los recursos, los gestores de incendios deben entender cuándo se presentan las ventanas de oportunidad para realizar quemas prescriptas, cómo estas varían a través del año, y cómo poder anticipar esas ventanas. Para dos tipos de quemas, en pilas y extendidas sobre suelo (*broadcast burn* en Inglés), caracterizamos las distribuciones temporales y espaciales de días propicios para quemar (*go-burn*), identificados mediante una base de datos de 15.468 permisos de quema, desde 2011 hasta 2024, del Centro de Coordinación del área geográfica del Norte de California. Determinamos la evolución temporal de las anomalías diarias a escala local y sinóptica de las variables ambientales que ocurrieron alrededor de dos semanas de iniciarse las quemas. Estimamos luego el número medio de ventanas históricas de prescripción para cada uno de los tipos de quema en cada mes, usando un abordaje novedoso para definir nuestro criterio de prescripción. Este abordaje define los criterios basados en rangos de condiciones ambientales presentes en los días propicios para quemar tomados del pasado en esa base de datos.

**Resultados** Las quemas extendidas o superficiales exhibieron una señal estacional muy fuerte de igniciones en junio y octubre. Las quemas en pilas, fueron cuatro veces más numerosas que las superficiales y ocurrieron más frecuentemente en noviembre y diciembre. La ubicación de las igniciones varió entre los meses y tipo de quema; por ejemplo, las pilas que se quemaron en el otoño ocurrieron en la Sierra, mientras que las pilas quemadas en la primavera lo fueron generalmente en la eco-región del piedemonte. Las variables ambientales tomadas en conjunto, y tanto a escalas sinóptica como local, indicaron ciertas preferencias en las quemas por algunas condiciones ambientales dependiendo del mes. Las condiciones que precedieron a las quemas superficiales realizadas en febrero, exhibieron temperaturas más elevadas y más secas cerca de la superficie y anomalías en los patrones de cuñas de altura en la alta atmósfera. Las quemas en pilas en octubre estuvieron asociadas con condiciones de superficies más frías y húmedas y patrones anómalos en la atmósfera. El número esperado de ventanas de prescripción de quemas varió debido al mes y al tipo de quema (por ejemplo, las ventanas de prescripción para realizar quemas prescriptas superficiales fueron, en promedio, tres veces más probables que las ventanas para quemar en pilas durante el mes de octubre).

**Conclusiones** Encontramos que una amplia posibilidad de oportunidades para realizar quemas prescriptas existe en el norte de California durante todo el año, aunque esas oportunidades dependen en gran medida del tipo de quema. Los resultados aquí presentados son útiles para determinar patrones de condiciones favorables que crean ventanas de prescripción de quemas, y para identificar ubicaciones prioritarias para implementar tanto quemas superficiales como en pilas.

## Background

Prescribed burns are effective tools to mitigate wildfire hazard and to restore ecosystem function in fire-adapted environments (Fernandes and Botelho 2003; Ryan et al. 2013; Hiers et al. 2020). These intentional burns are ignited by federal, state, local, and Tribal governments, private companies, and individual landowners. One goal is to reduce the volume and continuity of hazardous fuels in a controlled manner to curtail negative impacts of subsequent wildfires. In 2022, the United States Forest Service (USFS) released a 10-year Wildfire Crisis Strategy (USFS 2022), prompting a rapid increase in the planning of fuels treatments (i.e., thinning, prescribed fire, or both). The plan leverages partnerships across all levels of government with the goal to treat an additional ~ 50 million acres across the western US in high-risk "firesheds"–large (~ 250 k acres) landscapes identified to have a high likelihood of catastrophic wildfire impacts to homes, infrastructure, and municipal water supply (Evers et al. 2025).

Of the 271 high-risk firesheds across the contiguous US, the Geographic Area Coordination Center (GACC) in Northern California (ONCC) has the greatest number (49) of all GACCs. ONCC comprises northern California and the northwestern edge of Nevada and is characterized by complex terrain with 4000 m of topographic relief and nine ecoregions with varying landcover types (Fig. 1). Here, the ecoregions in Fig. 1b are used solely as aids for describing different locations across the region. This region exhibits a mid-latitude Mediterranean climate characterized by hot, dry summers and cool, moist winters. It displays notable interannual hydroclimate variability with wetter years interspersed with multi-year drought (Zamora-Reyes et al. 2022).

A comprehensive meta-analysis of over 40 treatment studies spanning 1994–2021 across the western US found that the most effective treatment strategy—a combination of thinning and prescribed pile or broadcast burning—reduced subsequent wildfire severity by 62–72% (Davis et al. 2024). Pile burning is defined as the ignition

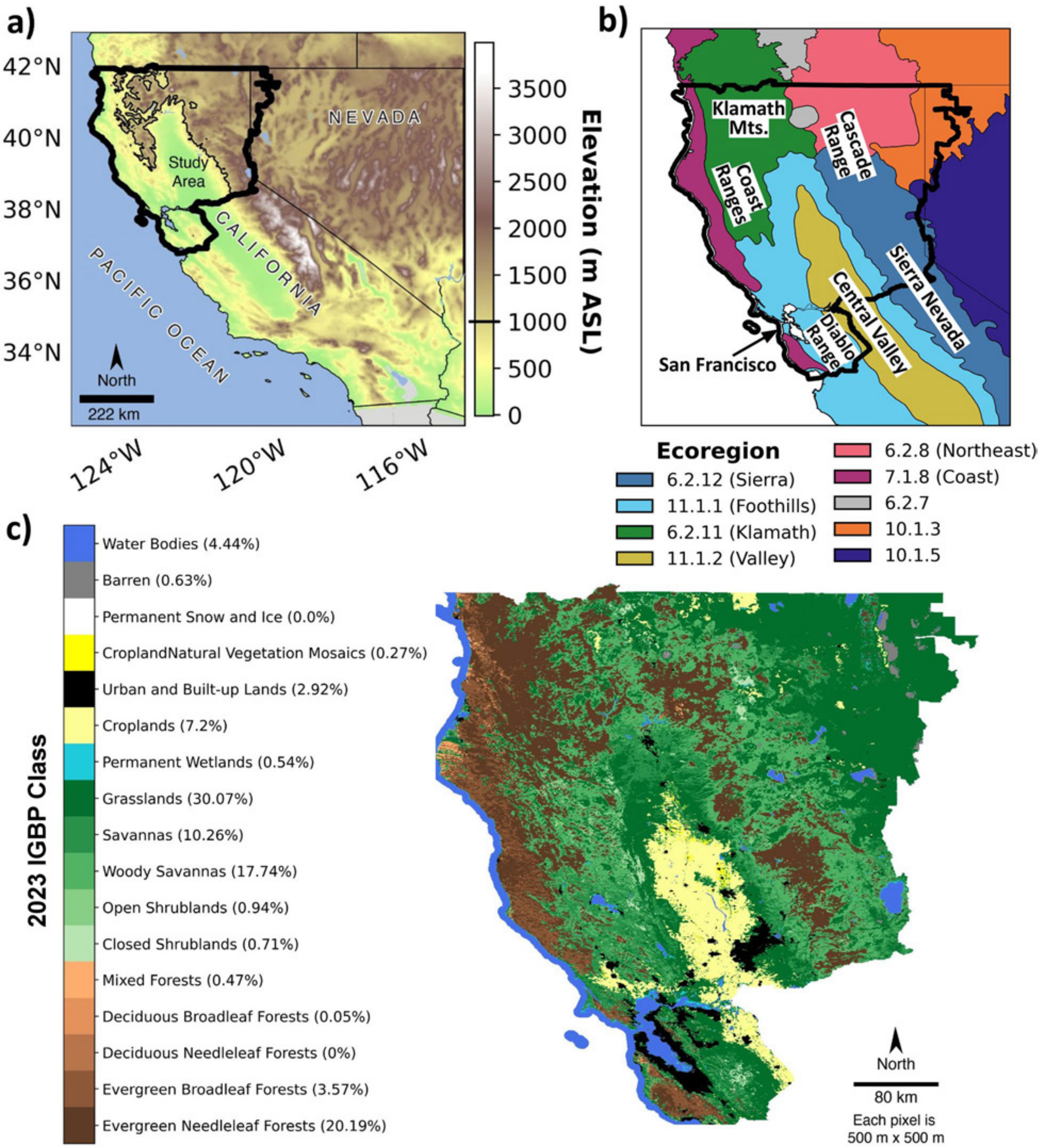


**Fig. 1** **a** Elevation (4-km resolution; from gridMET described in the Data section) and location (thick, black outline) of the Northern California GACC (ONCC) in the western US. The 1-km elevation level in ONCC discussed in the Methods section is indicated with a thin, black contour. **b** Environmental Protection Agency (EPA) Level III ecoregions (EPA 2012) within ONCC labeled with regional mountain ranges and reference points. Text in the legend indicates ecoregion aliases used throughout the paper. **c** 500-m International Geosphere-Biosphere Programme (IGBP) yearly land cover classes from the Moderate Resolution Imaging Spectroradiometer (MODIS) MCD12C1 Version 6.1 product (Friedl and Sulla-Menashe 2022) valid on 1 January 2023. The legend indicates the percentage of grid cells in ONCC with that classification

of one or many isolated piles of vegetative debris to remove larger fuels from a landscape. Hand-built piles are typically on the order of 2 $m^3$ (about 1.3 m on a side; Fig. 2a), but machine-built piles of slash can be much larger (upwards of 10–15 m on a side; Fig. 2b). Broadcast burning (Fig. 2c,d) more closely mimics natural wildfire behavior and is the practice of intentionally igniting fire on a predetermined plot of land (termed a “burn unit”). Various ignition patterns are employed to create desired fire behaviors in order to achieve intended fire effects within a burn unit, such as low-to-moderate intensity fire that consumes smaller fuel sizes but limits crown-scorch heights on mature trees. Broadcast burns are often simply referred to as “prescribed burns” in other regions of the country where pile burning is less common (e.g., the Southeast and the Great Plains). Here, we use prescribed burns as an umbrella term that includes both burn types, since both require a prescription of desired conditions to safely achieve objectives. It is worth noting that piles may be burned as part of a broadcast burn (Fig. 2e) and a pile burn may include some minor broadcast burning (Fig. 2f), but we explicitly refer to the specific fire type—broadcast or pile—in our analyses as both techniques are heavily used in northern California and typically one type is the focus of a burn permit. Given the high wildfire hazard in ONCC and known effectiveness of prescribed fire in reducing the chance of negative outcomes (e.g., large areas of high burn severity, extreme fire behavior, and structure loss), there is a critical need for research to support prescribed fire operations by characterizing weather conditions suitable for burning.

In California, conducting most prescribed burns requires several steps: (1) creation of a burn plan, (2) approval of a smoke-management plan (SMP) by the local air district, (3) unit preparation of the burn project, and (4) issuance of a burn permit by the local air district. Final approvals by fire agencies may also be necessary. The burn plan is a document developed weeks to years ahead of a planned burn and outlines the project location, fuels, objectives, staffing and equipment details, and contingency plans in the event of containment difficulties. The plan also outlines ranges of weather and fuels


**Fig. 2** **a** Spring season pile burning, Knights Valley, California. **b** Winter slash/machine-built pile burning, Mayacamas Mountains, California. **c** Early winter broadcast burning, Occidental, California. **d** Fall broadcast burning, Independence Lake, California. **e** Late fall broadcast burning that included some piles (center right), Glen Ellen, California. **f** Winter slash pile burning (pile in center) that included some broadcast burning to limit creeping spread of fire into adjacent unburned fuels, Mayacamas Mountains, California.

conditions, called "prescriptions," that must be in place before a burn is ignited. Prescriptions vary across plans, but include requirements for upper and lower bounds of temperature, wind speed, relative humidity, fuel moistures, and sometimes fire-danger indices from the USFS National Fire Danger Rating System (NFDRS; Deeming 1972; Deeming et al. 1977; Bradshaw et al. 1984; Jolly et al. 2024). Some cool-season plans for pile burns may require prescriptions for the presence of snow and a minimum snow depth, because continuous snow coverage can help meet the requirement for a continuous control line around the entire burn unit (e.g., NWCG 2018).

Even if a SMP is approved and weather and fuels fall within prescription, burns can still be postponed due to shortages of contingency wildfire suppression resources and a community's comfort level with a proposed burn (Toman et al. 2011; Quinn-Davidson and Varner 2012; Miller et al. 2020). For these reasons, decisions around prescribed burning are multi-faceted and require sophisticated planning and outreach (i.e., community engagement). Of all the reasons that may limit burning, weather and its impact on fuels is the biggest factor beyond human control. Therefore, improving our understanding of when environmental conditions meet specific criteria—so-called burn windows of opportunity, and herein referred to as "burn windows" or "burn days"—can support prescribed-fire planning and implementation.

Past studies have documented burn windows across several areas of the US. Weir et al. (2011) identified suitable opportunities for burning rangelands in Oklahoma based on criteria for temperature, relative humidity, wind speed, and precipitation. Using these same criteria, Yurkonis et al. (2019) identified weather windows for grassland burning in the northern Great Plains using observations from 20 weather stations across North Dakota and Minnesota. Chiodi et al. (2018) performed a similar analysis for the Southeast US, but using prescription guidelines developed specifically for prescribed burning in the southern US (Wade and Lunsford, 1989). Chiodi et al. (2018) used reanalysis weather datasets and an expanded set of criteria including the aforementioned variables as well as mixing height and transport wind (defined in the Data section), which influences smoke dispersion and transport.

Few studies have explored burn windows for California and none have documented the large-scale weather patterns associated with prescribed burns, nor have they examined the differences in conditions based on the prescribed burn type. Baijnath-Rodino et al. (2022) estimated the number of burn windows in California, but windows were based on satisfying prescription criteria developed for prescribed burning in forested ecosystems in the southern US (Wade and Lunsford, 1989) using a limited set of parameters (daily maximum and minimum temperature, daily minimum relative humidity, and daily average wind speed). Swain et al. (2023) defined burn windows based on satisfying prescription criteria generated from compiling 22 historical burn plans. However, the burn plans were collected from projects that spanned the entire western US and were therefore not representative of the weather and vegetation types encountered in ONCC. These studies quantified the number of burn windows (without accounting for different burn types) on a seasonal basis with a focus on how that number has shifted over time or is expected to shift in the future.

The scope of our work is differentiating between broadcast and pile burns on sub-seasonal timescales to (1) characterize the temporal and spatial distributions of past burn occurrences across ONCC, (2) identify the average local- and synoptic-scale weather patterns typically associated with past ignition days each month, and (3) quantify the average number of burn windows each month. We report averages in this paper as the geometric mean. To identify the burn windows, we implement a novel retrospective approach to define the ranges of typical burn conditions associated with past burns. Specifically, we use coincident prescribed burn and environmental data from past "go-burn" days to inform prescription thresholds under which a prescribed fire may be ignited in various elevation and landcover types in ONCC. Our assumption is that for at least some hours of the day, the conditions on past burn days were within or sufficiently near the prescription criteria in the official burn plans. We also provide insights for planning and management decisions that can aid in increased implementation of prescribed fire operations in ONCC.

## Data

### Prescribed fire data

We collected 14 years (2011–2024) of prescribed fire data from the Prescribed Fire Incident Reporting System (PFIRS). PFIRS is an interface between individuals or entities that want to burn in California and air-quality managers who issue prior approvals. Title 17 of the California Code of Regulations (Title 17, 2001) requires submission and approval of SMPs and issuance of a burn permit to conduct most prescribed burns exceeding 0.01 acres. Some local air districts only require burn permits if the project size exceeds 10 acres or is estimated to produce more than 1 ton of particulate matter. For these reasons, the PFIRS dataset underestimates burns, including agricultural burns, that are < 10 acres, which are most likely conducted by individuals and private companies. PFIRS data include the ignition date, representative coordinates of the burn project, requesting entity, area burned, and burn type.

These data are typically entered into the system before the burn takes place, with the exception of the burned area, which is populated after the burn occurs. To focus on days with no known containment issues, we used the dataset produced by Li et al. (2025) to identify and remove any escaped prescribed fires. If a fire occurred on the same day and within a 10-km radius of a fire listed in Li et al. (2025), it was removed: six such fires were removed.

Our analysis focuses on prescribed fires in three predominant vegetation types in ONCC: (1) grass, savanna, or shrub (GSS, 59.7%), (2) forest (24.3%), and (3) croplands (7.5%) (percentages based on the 2023 landcover data in Fig. 1c). These categories were chosen to broadly capture the characteristic ecosystems that people burn in to achieve different objectives. While the PFIRS dataset does not contain information about a burn's objectives, we know that practitioners burn in GSS to achieve ecological benefits such as rangeland improvement, reduction of thatch and invasive species, and to manage encroachment of *Baccharis pilularis* (coyotebrush shrub) onto coastal prairies (Yurkonis et al. 2019, Hopkinson et al. 2020, Keeley et al. 2023, Noda et al. 2025, Kjaer et al. 2025). Burns in forested areas are often conducted to reduce wildfire risk via hazardous fuel reduction and restoration of natural fire regimes (Vaillant et al. 2009; Knapp et al. 2017). On the other hand, cropland or agricultural burns in California are used for pest control, weed abatement along ditches, and removal of post-harvest debris such as orchard or grape vine prunings and rice stubble (Bahardar 1993, CARB 2026). Operationally, the fuels within these broad ecosystem types inform resource requirements (staffing and the type of unit preparation) and contingency planning based on potential fire behavior concerns if fire were to escape the unit.

We also analyze the following two burn-type categories: (1) entries labeled as machine, hand, or landing pile in the PFIRS data were classified as pile burns and (2) entries labeled as broadcast burns were classified as such. In practice, under favorable conditions, these types may not be mutually exclusive (e.g., Fig. 2e and f). However, we assume that the primary burn type is the one stated in the burn permit. We discarded 1,350 entries with unknown burn types or that were outside of our vegetation classes, resulting in a final count of 15,468 prescribed fires in our PFIRS subset. Lastly, we grouped requesting entities into six categories: Federal government; State/County/Local government; Tribal government; Private; Individual land owner; and Unknown. The State/County/Local government category included entities like local fire departments and water municipalities. The Private category included companies, non-governmental organizations, and universities.

#### Local- and synoptic-scale environmental data

To assess local conditions, we use weather, fuel-moisture, and fire-indicator variables from the gridMET high-resolution, surface meteorological dataset (Abatzoglou 2011). This dataset contains once-daily variables constructed from blending high spatial resolution data from Parameter-elevation Regressions on Independent Slopes Model (PRISM; Daly et al. 2008) with high temporal resolution data from the North American Land Data Assimilation System Phase 2 (NLDAS-2) regional reanalysis (Mitchell et al. 2004). The result is a gridded dataset of fire-relevant variables over the contiguous US spanning 1979–present at 1/24° (~4 km) horizontal grid spacing. Daily gridMET quantities are derived from a 24-hour period starting at 0700 UTC. We downloaded daily maximum temperature (max-t), daily minimum relative humidity (min-rh), 24-hour precipitation accumulation (total-precip24hr), daily average 100-hour and 1000-hour dead fuel moisture content (avg-DFM100hr, avg-DFM1000hr), and the daily average Burning Index-G (avg-BI for fuel model G) for the ONCC domain. The 100-hour (1000-hour) timelag corresponds to the amount of time for 1–3" (3–8") diameter fuels to change the moisture content of >66% of their mass in response to changes in atmospheric conditions (Carlson et al. 2007). BI indicates expected containment difficulty when accounting for fire intensity and spread (Bradshaw et al. 1984). Calculations for fuel moisture content and BI are based on the NFDRS version 3 (Deeming et al. 1977).

gridMET only offers daily average wind speeds, which may dilute the magnitudes experienced during the daylight hours when prescribed burns typically occur (Chiodi et al. 2018; Yurkonis et al. 2019). Instead, u- and v-wind components from 3-hourly, 0.25° (~27 km) ERA5 reanalyses data (Hersbach et al. 2020, 2023a) are used to calculate daily daylight-average wind speeds (avg-wspd) at 10 m above ground level (AGL). We define daylight hours between 1800UTC and 0000UTC (10AM–4PM Pacific Standard Time, following Chiodi et al. 2018). We also processed variables relevant for estimating the daily daylight-maximum ventilation index (max-vi), a critical indicator to estimate the transport and dispersion of smoke emitted from prescribed fires (Hardy et al. 2001; Chiodi et al. 2018). vi at time *t* is calculated as:

$$\mathrm{vi_t} = \mathrm{mh_t} \times \mathrm{transwspd_t} \tag{1}$$

where mh (m AGL) is the mixing height defined as the depth above ground that ground-released pollutants will vertically disperse (Fearon et al. 2015) and tranwspd (m

$s^{-1}$) is the transport wind defined as the vertical average of the wind speed in the column of air near the ground and mh (Hardy et al. 2001). Details of how we calculated mh and transwspd from ERA5 single- and pressure-level data (Hersbach et al. 2023a, 2023b) are provided in Additional file 1. Herein, max-vi ($m^2s^{-1}$) is the maximum of Eq. (1) during daylight hours. The ERA5 variables were bilinearly interpolated to match the 4-km gridMET domain.

All local variables were obtained for 2005–2024 over the ONCC domain to cover the PFIRS period of record and to construct long-term means. To assess synoptic-scale atmospheric circulation patterns associated with the prescribed fires, we use daily average, 0.25° 500 hPa (z500) geopotential height data from ERA5 over 180° W–60° W longitude and 25° N–70° N latitude.

## Methods

### Calculating composites of standardized anomalies of local weather variables for past prescribed fires

We extract data for each past prescribed fire by bilinearly interpolating our daily max-t, min-rh, avg-wspd, total-precip24hr, max-vi, avg-DFM100hr, avg-DFM1000hr, and avg-BI fields to the fire's location (e.g., 40.498° N, 122.399° W) on ignition day. We then calculate the standardized anomaly for each fire and each variable by subtracting the corresponding long-term mean and dividing by the corresponding long-term standard deviation. We calculate the mean and standard deviation using data at the fire's location within a buffer window of ± 3 days surrounding each ignition day for the years 2005–2024 (~140 samples per burn). The buffer window is used to create a sliding 7-day window of data centered around each day in order to increase the sample size and to smooth out small variations in the long-term mean and standard deviation. We also tested a 30-year (1995–2024) and a 14-year (2011–2024; consistent with the prescribed fire record) period, but did not see substantial differences in preliminary results (not shown). We used the 2005–2024 period to achieve a balance between large enough sample sizes and being able to put prescribed fire conditions in the context of a contemporary climatology. We then repeated the same procedures to calculate standardized anomalies for each day in the 7 days before and after ignition day.

To calculate composites of the daily standardized anomalies for each variable, we aggregate then average the daily standardized anomalies of all pile or broadcast burns that occurred across ONCC in a given month. When multiple fires of the same burn type occurred in ONCC on the same day, we used the average of the standardized anomalies across all fires of the same type on that day to avoid duplicate days in our monthly composite. Composites for a particular month were not calculated if the number of unique days for the month's composite was less than 5% of the total number of unique days across all months for the burn type. For pile (broadcast) burns, this translated to at least 99 (66) unique days to construct a monthly composite.

### Calculating composites of synoptic-scale anomalies for past prescribed fires

For z500, we calculate the anomaly from the 2005 to 2024 long-term mean for all grid cells. We then compute averages of daily z500 anomalies separately for pile and broadcast burns for each month. For example, we calculated the average anomaly on all ignition days when a pile burn occurred anywhere in ONCC for each month to create a monthly pile composite map. In the event that multiple pile burns occurred in ONCC on a given day, we only included the z500 anomaly for that day once to avoid duplicate days.

We also create Hovmöller diagrams (Persson 2017), time-longitude diagrams that depict variations in the temporal-spatial structure of a variable that has been averaged over a representative latitudinal band. We use them to illustrate how the monthly composite of daily z500 anomalies evolved near ONCC in the time before and after past ignition days. Here, we calculated the latitudinal average of the monthly composite of daily z500 anomalies between 30° and 60° N separately for each day in the 2 weeks centered on ignition day.

### Determining "typical burn conditions" and burn windows of opportunity

We used full-field variables to define what we refer to as the "typical burn conditions" of ONCC prescribed fires, which will be used to identify the number of burn windows. Our approach is as follows: we first aggregate all past burns in our PFIRS subset into subgroups. The subgroups bin past fires based on their burn type, ignition month, elevation band, and characteristic vegetation. We use 3-month sliding windows centered around each month-of-interest so that typical burn conditions are generated separately for each month (e.g., typical burn conditions for June broadcast burns were defined based on broadcast burns that were ignited in May-June-July). A 3-month window was used to increase the sample sizes within the subgroups and to allow for a wider range of conditions that realistically could occur in the month of interest (e.g., it is plausible to experience May-like prescribed burn conditions in June). We use this month-specific approach (with the ± 1-month buffer) rather than defining one set of typical burn conditions for the entire year. The latter would create very wide ranges that discount the fact that some months never experience conditions near the bounds, ultimately making it difficult for practitioners to disentangle what realistic ranges are for a specific time-of-year.

Subgroups for vegetation were based on whether the fire occurred in GSS, forest, or crop according to the corresponding year's observed landcover (see Fig. 1c) using nearest neighbor resampling from the 500-m landcover grid. Subgroups for elevation were based on whether the fire occurred ≤ 1 km or > 1 km ASL. The 1-km threshold was selected to separate lower-elevation burns in the valley and lower foothills from those in the high mountains (Fig. 1a). Many air districts make burn approval decisions based on a similar demarcation (~ 914 m ASL) (Title 17, 2001). For the crop class, we only create a ≤ 1 km elevation subgroup, since crop burns at elevations > 1 km are limited.

For each burn in each subgroup, we then extract daily environmental variables by bilinearly interpolating to the location of all burns in the subgroup, thereby creating an empirical distribution for each variable and subgroup. From these distributions, we take the 5th and 95th percentiles to define the bounds of each variable that constitute the "typical burn conditions." We selected these percentiles to capture the majority (90%) of conditions that practitioners ignited under while excluding the most rare conditions. We believe this provides a reasonably wide range for "go-burn" decisions, but we acknowledge that it is possible to ignite under conditions at the edges of the distribution, sometimes as a necessity to achieve particular project objectives. Therefore, we provided complementary results in Additional file 2 using conditions criteria based on the minima and maxima (i.e., 0th and 100th percentiles) of the distributions.

We used most of the local variables listed in the Data section (i.e., daily max-t, min-rh, avg-wspd, max-vi, avg-DFM100hr, avg-DFM1000hr, and avg-BI) to define our typical burn conditions. However, instead of total-precip24hr, we calculated the number of days since wetting precipitation (≥ 2.54 mm/day; days_since_wp; Holden et al. 2018), including snow (as meltwater). This variable better accounts for the effect of precipitation on soil, duff, and fuel moistures in the time leading up to ignition day. We used days_since_wp in lieu of snow depth, because it is an applicable prescription variable for both burn types and it accounts for wetting effects from any precipitation during either the warm or cool season. Snow depth can be measured on site (if it is part of a prescription), but station-based records of snow depth, and as a result, gridded snow depth products, are subject to larger uncertainties and many limitations. However, exploring the presence and depth of snow during pile burning is worth future investigation to assess how commonly snow is potentially leveraged to provide a barrier to fire spread. Examples of variable distributions and associated thresholds used to define typical burn conditions for June broadcast burns in each vegetation-elevation subgroup are shown in Fig. 3. We do not define typical burn conditions for any subgroups with fewer than 10 samples. Distributions and conditions criteria for pile burns and all other months are provided in Additional file 3.

In this study, a burn window/day occurs when conditions on a given day at a given 4-km grid cell simultaneously fall within all of the variables' 5th and 95th percentiles (or minima-maxima for figures in Additional file 2) for that grid cell's vegetation-elevation subgroup. Figure 4 shows the locations of the five vegetation-elevation subgroups in ONCC used for determining burn windows in 2023. Using data from the most recent 20 years (2005–2024), we tabulate the number of days per month that satisfy typical burn conditions then calculate the mean over this period to determine the mean number of burn windows for each month. We performed the calculations separately for each gridMET grid cell in ONCC (Fig. 4).

Prescribed fires can burn in a variety of environmental conditions, including those that may never occur in ONCC or have not been captured in our analysis, since our criteria for typical burn conditions is derived solely from conditions associated with past burns. We see this caveat as an advantage because this means that our criteria for burn windows are based on when burn practitioners decided it was an opportune time to perform burns. The aforementioned analysis using our definition of burn criteria can therefore be interpreted as follows: if burn practitioners in ONCC burn as they have in the past, under the conditions that are available to them in ONCC, these are the average number of days that we can expect to meet burn conditions each month.

#### Evaluation of statistical significance

To estimate the likelihood of obtaining our results beyond random chance, we use bootstrapping (Efron 1979; Wilks 2011) to construct a distribution around our statistical metrics. This entails recalculation of a metric 10,000 times, each with a new batch of data that were randomly resampled, with replacement, from the original set of values used to calculate the metric. If the metric falls below the 0.025 or above the 0.975 quantile of the bootstrapped distribution (a two-sided $p$-value < 0.05), we conclude that it is unlikely (<5% chance) that the metric is a result of random chance.

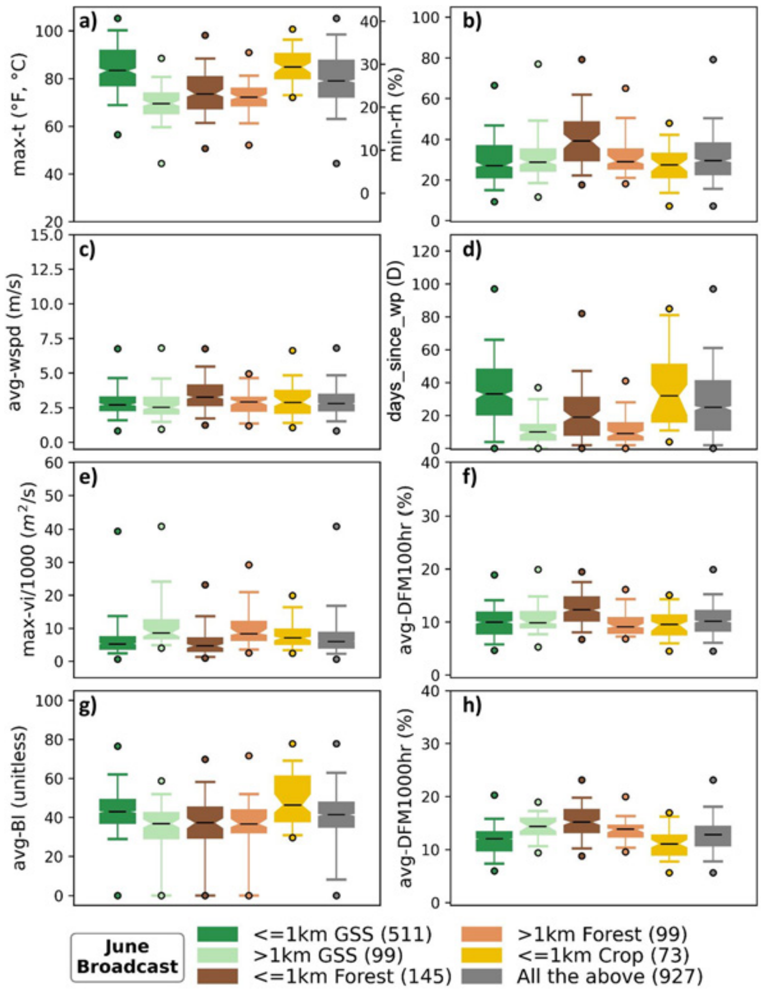


**Fig. 3** Notched boxplots of variable distributions (**a–h**) used to define the typical conditions for June broadcast burns. Each of the vegetation-elevation subgroups is indicated by the legend; parentheses indicate the number of samples. Gray boxplots show the distributions when combining all vegetation-elevation subgroups. Dots represent the minima and maxima and black, horizontal lines indicate the medians of the distributions. Whiskers indicate the bounds of the typical burn-day conditions (i.e., 5th and 95th percentiles of the distributions). Figures for both burn types for the remaining months are in Additional file 3

## Results

### Temporal distribution of past burns

#### *Broadcast burns*

Within our PFIRS subset, there were 3,174 broadcast burns for a total of 183,484 acres treated during the 2011–2024 period in ONCC. Broadcast burning has generally increased in ONCC; only 3 years (2014, 2021, 2024) had a decrease in the annual area treated over the prior year (right-side histogram in Fig. 5a). Nearly half (48.5%) of the area treated with broadcast burns in the 14-year period occurred in the last 3 years alone, highlighting the impact of the 2022 Wildfire Crisis Strategy. Federal agencies consistently held the largest share of yearly treated area, except for 2024, when State/County/Local government agencies burned ~25.3% more than federal agencies. The daily frequency of occurrence and area treated by broadcast burns (color shading and top gray histograms in Fig. 5a, respectively) show strong seasonal signals. There is a broad cluster of burning that expands from late January through the end of June; then there are few burns in July through mid-September; burn activity then increases again, peaking in October and then steadily tapering off through mid-December. Spring (March-April-May) had the greatest percentage of ignitions (32.5% of total). However, the single months with the greatest occurrence of ignitions were June (16.4%) and October (15.3%). The fact that single months can have some of the greatest ignition counts and area treated, while the season that they fall into does not, highlights the importance of analyzing prescribed fires

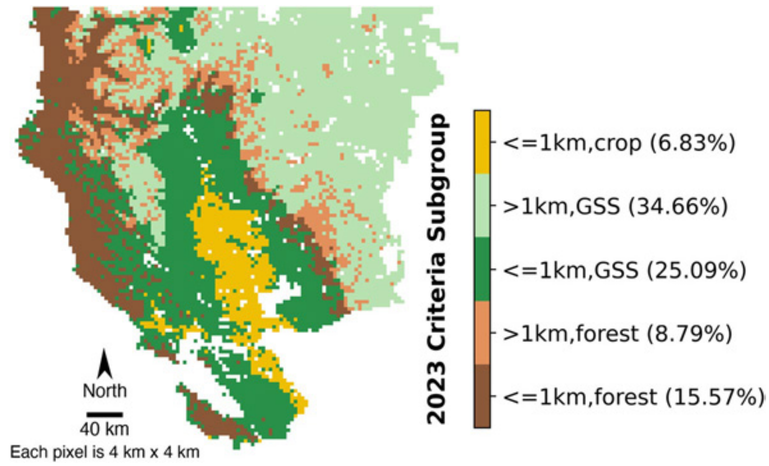


**Fig. 4** Example locations of vegetation-elevation subgroups used for identifying burn windows. The legend represents the percentage of 4-km gridMET grid cells in ONCC within each subgroup. Grid cells are masked if they do not fall into any of the subgroups. The underlying elevation data are from gridMET and the vegetation data are from the MODIS MCD12C1 Version 6.1 product (Friedl and Sulla-Menashe 2022) valid on 1 January 2023 and regridded from 500 m to 4 km using nearest neighbor interpolation to match the gridMET domain

on sub-seasonal timescales. Some seasons have a combination of very active and inactive months (e.g., June-July-August or September-October-November), which may obscure the importance of more granular weather conditions and operational considerations to conduct burns within those seasons.

#### *Pile burns*

There are nearly four times as many pile burns (12,294) in our PFIRS subset than broadcast burns, yet the area treated by piles (183,821 acres) is nearly the same. Only 4 years (2013, 2017, 2018, 2024) had a decrease in annual area treated over the prior year (right-side histogram in Fig. 5b) and nearly half (45.6%) of the total area treated with pile burns has been done in the last 3 years alone. Distinct from broadcast burning, private companies have consistently contributed to a relatively large proportion of the annual area treated with pile burns up until 2021 (gold portion in right-side histogram in Fig. 5b). Since 2021, the annual area treated by governmental agencies has taken on an outsized share (i.e., governmental agencies treated, on average, 9.5 times more area per year than private companies). The daily frequency of occurrence and area treated by pile burns (color shading and top gray histograms in Fig. 5b, respectively) show a broad cluster extending from early October through May. Few pile fires occurred in June–September, while winter (December–February) accounted for nearly half (48.9%) of all ignitions. December (21.2%) and November (20.1%) saw the greatest number of ignitions.

### Spatial distribution of past burns

#### *Broadcast burns*

Spatial plots in Fig. 6 (1st and 3rd columns) reveal locations of past burns seasonally distributed across ONCC as a function of vegetation type, with the stacked bar charts in Fig. 6 (2nd and 4th columns) providing a breakdown of the monthly proportion of burns in each ecoregion. Generally, past burns of both types were ignited around all sides of the Valley, within GSS and croplands in the Valley, extending north across the Klamath Mountains, and westward to coastal forests north and south of San Francisco. 94.4% of the 3,174 broadcast burns occurred in five of the nine possible ONCC ecoregions (see Fig. 1b): Foothills (41.0%), Sierras (27.3%), Coast (9.0%), Valley (9.0%), and Klamath (8.1%). Broadcast burns are most common in the Foothills every month outside of fall (September–November); burns in the fall are more evenly distributed across ecoregions. Broadcast burning in the Valley occurs in most months but represents its largest proportion in June and September around spring and fall harvest of croplands (yellow dots in first column of Fig. 6).

#### *Pile burns*

Pile burns occurred across all nine ecoregions in ONCC, but 96.1% of the 12,294 pile fires occurred predominantly in four ecoregions throughout the year: Sierra (45.0%), Foothills (29.7%), Klamath (15.6%), and Coast (5.8%). In the fall and winter months (September–February) and June, pile burns are most common in the Sierra, while burns in the spring months (March–May) and August are most common in the Foothills (Fig. 6, fourth column).

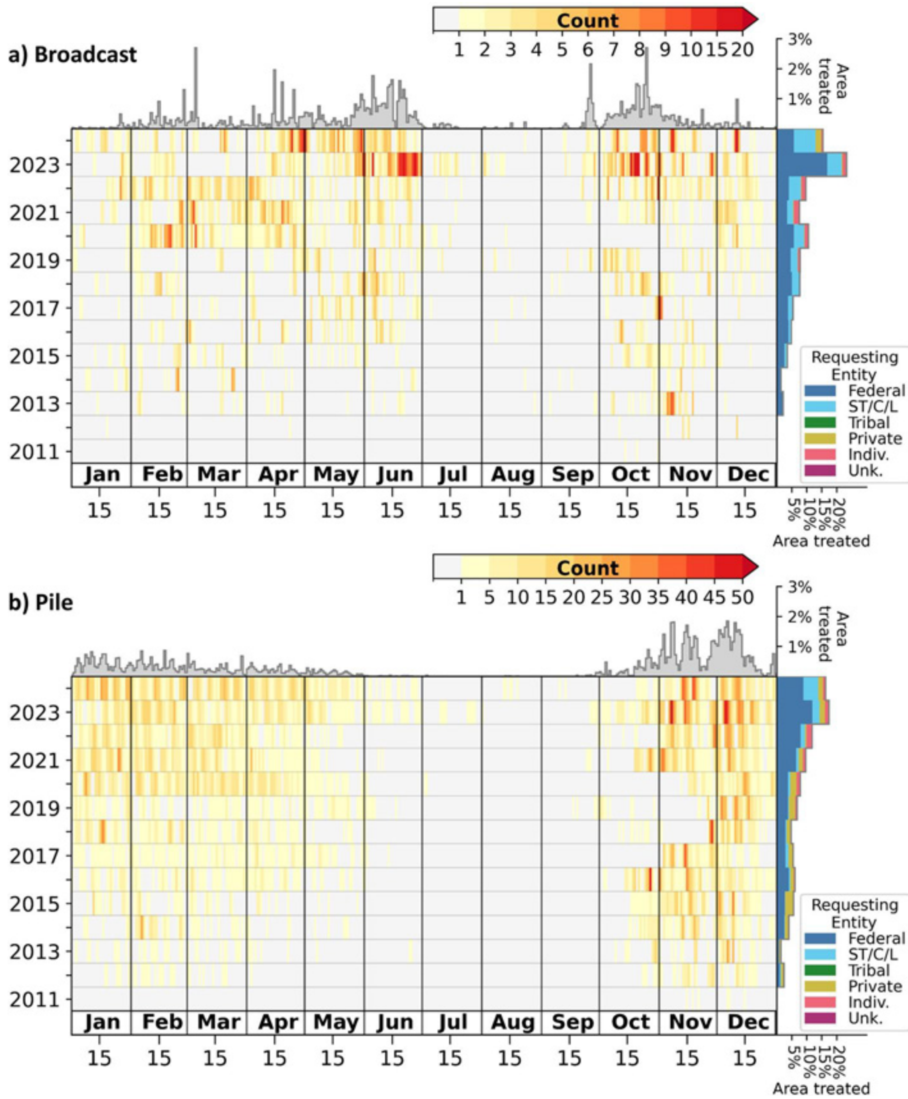


**Fig. 5** Count (yellow–red colorbars) of the number of past prescribed burns in our PFIRS subset within ONCC on each day (horizontal axes) for each year (vertical axes) between 2011 and 2024. The 15th day of each month is marked. Gray histograms on top of the subplots indicate the percent of the total area treated between 2011 and 2024 by prescribed burns on any given day. Histograms on the right side of the subplots indicate the percent of the total area treated between 2011 and 2024 by prescribed burns each year. Color-shading within the right-side histograms represents the yearly proportion of area treated by each requesting entity (see Data section). ST/C/L stands for State/County/Local government. Broadcast burns are in **a** and pile burns in **b**. Note the change in colorbar scale between the two fire types

Pile burning in the Klamath does not make up the majority of burning in any month, but the greatest monthly proportion of burns there occur in the cooler months October–January. The warmest months of the year, June–September, have few pile burns compared to the other months; but of the burns that occurred, a sizable percentage (~17–67% depending on the month) occurred in the Coast ecoregion, presumably due to relatively cool and moist conditions making it possible to conduct burns more safely for the time of year. Use of piles any month of the year for burning croplands in the Valley was negligible (<0.5% of pile burns).

### Local weather characteristics of past burns

In order to characterize how anomalous the local conditions associated with past prescribed fires are with respect to climatology, we calculated monthly composites of daily standardized anomalies for each day in the ± 7 days surrounding past ignition days according to the procedures outlined in the first subsection of the Methods.

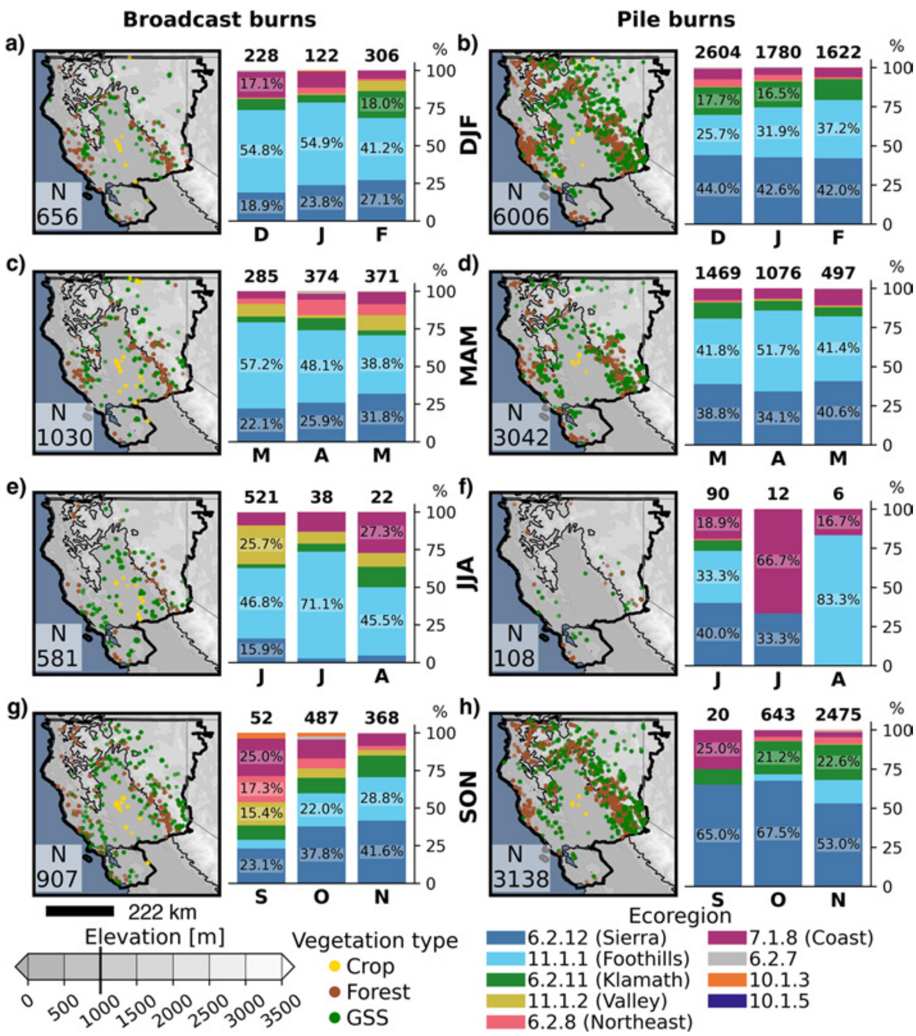


**Fig. 6** Maps of the spatial distribution of individual past broadcast burns (1st column) and pile burns (3rd column) in our PFIRS subset in ONCC during each meteorological season (rows). Fires are color-coded according to the vegetation type (grass/savanna/shrub (GSS), forest, or crop) at that location. "N" is the total number of fires within the season for that fire type. gridMET elevation and the 1-km contour discussed in the Methods section are underlaid according to the colorbar. Neighboring bar charts show the percentage of prescribed fires in each month that occurred in each ecoregion plotted in Fig. 1b. Annotations for percentages > 15% are shown. Bolded numbers at the top of each bar indicate the total number of past fires within that month

#### *Anomalous conditions before, during, and after past broadcast and pile burns*

The average local conditions associated with broadcast burns exhibit variations in their significance from the long-term mean base on the month (Fig. 7). In the cool months (November–April), we see patterns of past environmental preferences by burn practitioners that are unlikely due to random chance; max-t and avg-BI are generally above normal in the days leading up to and including ignition day (orange streaks in Fig. 7). Simultaneously, min-rh, total-precip24hr, avg-DFM100hr, and avg-DFM1000hr are below normal in the days preceding ignitions, indicating a slightly drier environment. DFM1000hr, by definition, changes minimally over 2 weeks, so the "dry streak" during these months indicates that a persistent fuel moisture deficit is typically needed for larger fuels to be receptive in a typically cool and wet time of year. Anomaly patterns after ignition are relatively weaker and less consistent than preceding patterns, except for avg-DFM1000hr. Monthly composites of daily standardized anomalies during past pile burns in ONCC exhibit some preference for a cooler and wetter pattern (darker blues and greens around ignition days in Fig. 8) to conduct pile burning in May and in the fall that is unlikely due to random chance.

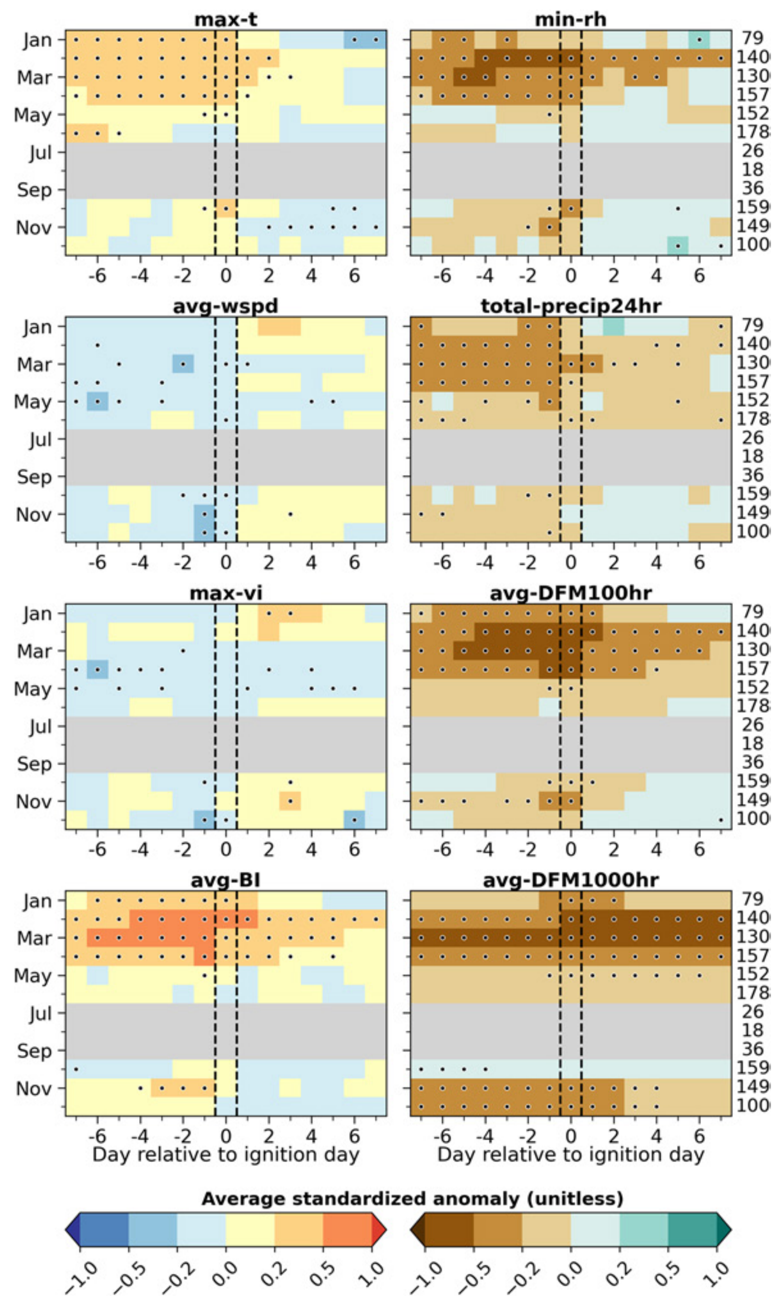


**Fig. 7** Averages (means) of daily standardized anomalies for past broadcast burns in ONCC organized by month (vertical axes). Results are shown for each day in a window of ± 7 days surrounding ignition day (horizontal axes) and for the set of fire weather (max-t, avg-wspd, min-rh, total-precip24hr), fuel moisture (avg-DFM100hr, avg-DFM1000hr), fire danger indicator (avg-BI), and smoke-relevant (max-vi) variables. Moisture quantities are displayed with a brown-green colorbar to aid in interpretability. Black, dashed lines bound the ignition day. Dots indicate that the plotted result is unlikely to have occurred by random chance at the 5% significance level using 10,000 bootstrapped samples with replacement. Numbers to the right of the plot indicate the number of samples in each monthly composite. The gray mask indicates that there were too few samples to construct a monthly composite (see first subsection of the Methods)

### Synoptic weather characteristics of past burns

We characterize synoptic-scale conditions associated with past burns by calculating composites of daily z500 anomalies for each month, using the procedures outlined in the second subsection of the Methods. We first show composites for ignition day and then show Hovmöller diagrams to illustrate how the composite anomalies evolved in the ± 7 days surrounding ignition.

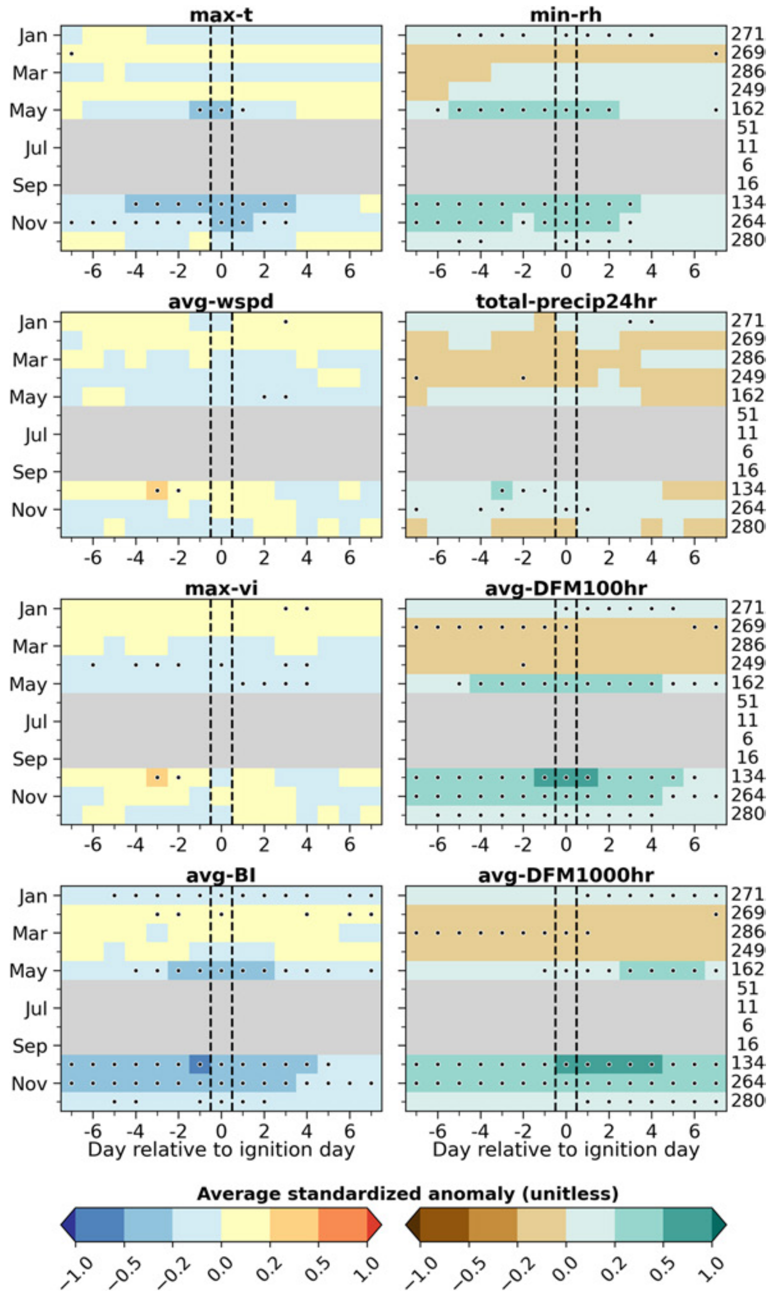


**Fig. 8** Same as Fig. 7, but for past pile burns

***Anomalous conditions before, during, and after past broadcast burns***

Recall composites of the local-scale conditions showed persistent anomalies that evolved over time (Figs. 7 and 8). These patterns motivate investigation into the large-scale weather systems in the form of troughs and ridges that may be influencing the local conditions encountered at past prescribed-fire locations. As such, Fig. 9a and b show the average of the daily z500 anomalies associated with past broadcast burns ignited in February and June, respectively. February is selected because the local composites in Fig. 7 showed relatively strong anomalies. June is selected because it is the most popular month (by count and area treated) for broadcast burning in our PFIRS subset.

February results show anticyclonic anomalies, indicative of a relatively strong and broad upper-level ridge (positive anomalies in Fig. 9a). The ridge is typically

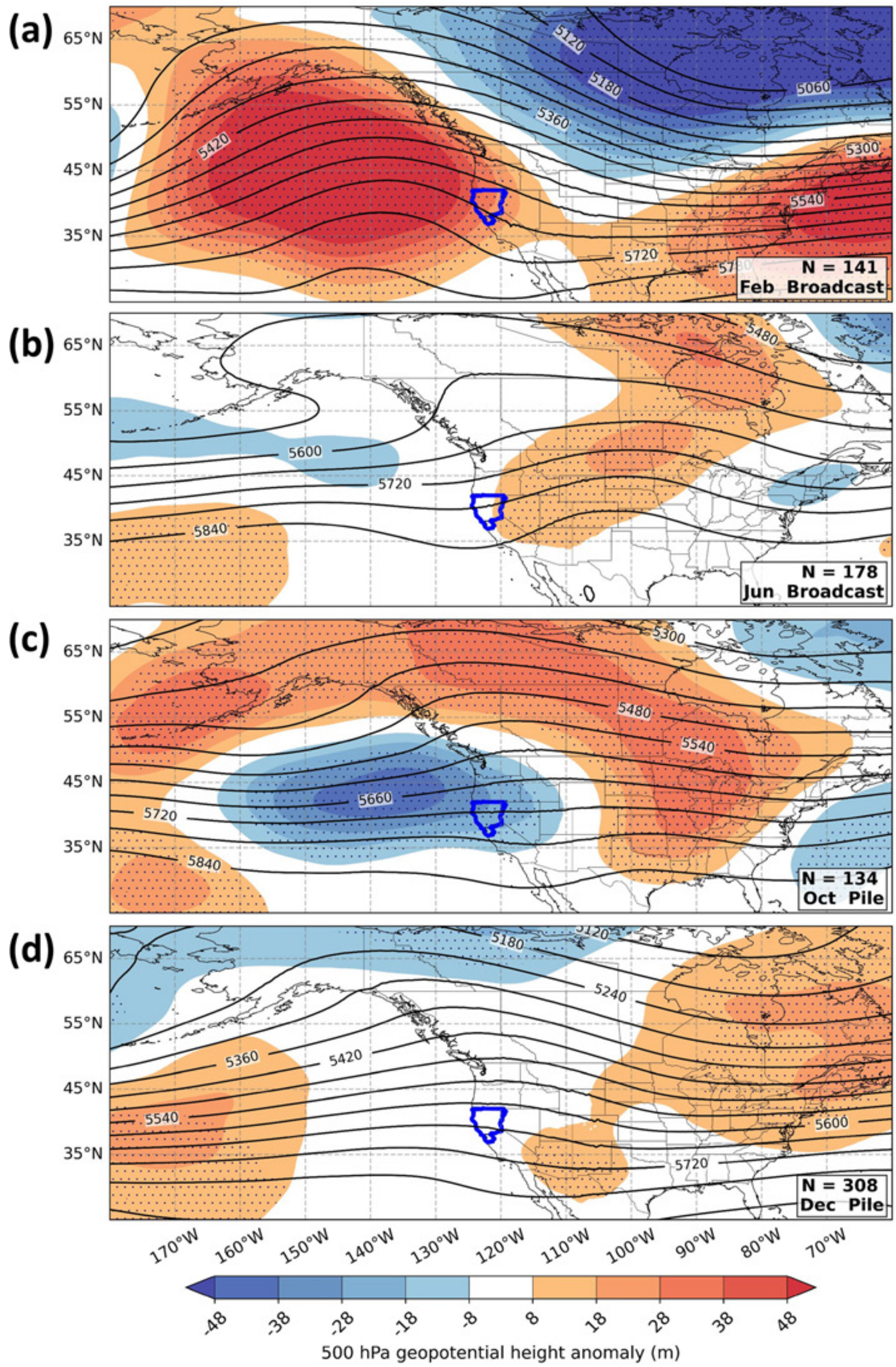


**Fig. 9** Composite of daily z500 anomalies associated with the ignition day of past **a**,**b** broadcast burns and **c**,**d** pile burns that occurred in ONCC (thick, blue outlined polygon) from 2011 to 2024 organized by month: **a** February, **b** June, **c** October, and **d** December. Solid contour lines show the composite z500 value at 60-m intervals. Stippling indicates that the plotted result is unlikely to have occurred by random chance at the 5% significance level using 10,000 bootstrapped samples with replacement. Figures for remaining months are in Additional file 4

positioned south of British Columbia, Canada in the Northern Pacific Ocean and extends south over ONCC on the day of ignition. The strongest positive anomalies are located just off of the coast; this signal is attributed to strong agreement (78%) for positive anomalies among the composite samples (not shown). Areas ahead of and under a ridge axis typically experience few clouds, higher temperatures, and lower relative humidities, all favorable conditions for increasing fuel receptivity in an otherwise cool and wet month of the year. These characteristics are indeed consistent with the local conditions that we found for broadcast burns in our PFIRS subset in February (Fig. 7).

We use Hovmöller diagrams to show the temporal evolution of the anomaly patterns at each longitude. First, the ignition-day patterns in Fig. 9 are averaged over a representative latitudinal band across ONCC. This flattens the composite maps in Fig. 9 into a one-dimensional array, where each longitude is assigned one value. We repeat this process for the composites associated with each day in the week before and after ignition day to create a two-dimensional plot of longitudes (horizontal axis) by time (vertical axis). As a result, the diagrams show how the patterns evolve over time in relation to ONCC's longitudinal location. For instance, reading from the top to the bottom of the vertical axis of Fig. 10a, we see that the positive anomalies over ONCC (between the blue dashed lines) persist during the week ahead of broadcast ignitions. This pattern begins to retreat offshore as the area of negative anomalies over the central US shifts further southwest within 4 days of ignition. This persistence (i.e., consistent anomaly at a given longitude) indicates very little longitudinal movement of the amplified ridge pattern in the week ahead of broadcast ignitions in February, which contributes to enhanced warming and drying of fuels in ONCC. The stippling dots indicate statistical significance of the pattern (see Fig. 10 caption).

In contrast, June results show no systematic preference for anomalous large-scale patterns near ONCC on broadcast ignition days (Fig. 9b) other than slight ridging to the east over the Great Basin and upper central US. The lack of pattern over ONCC is attributed to weaker

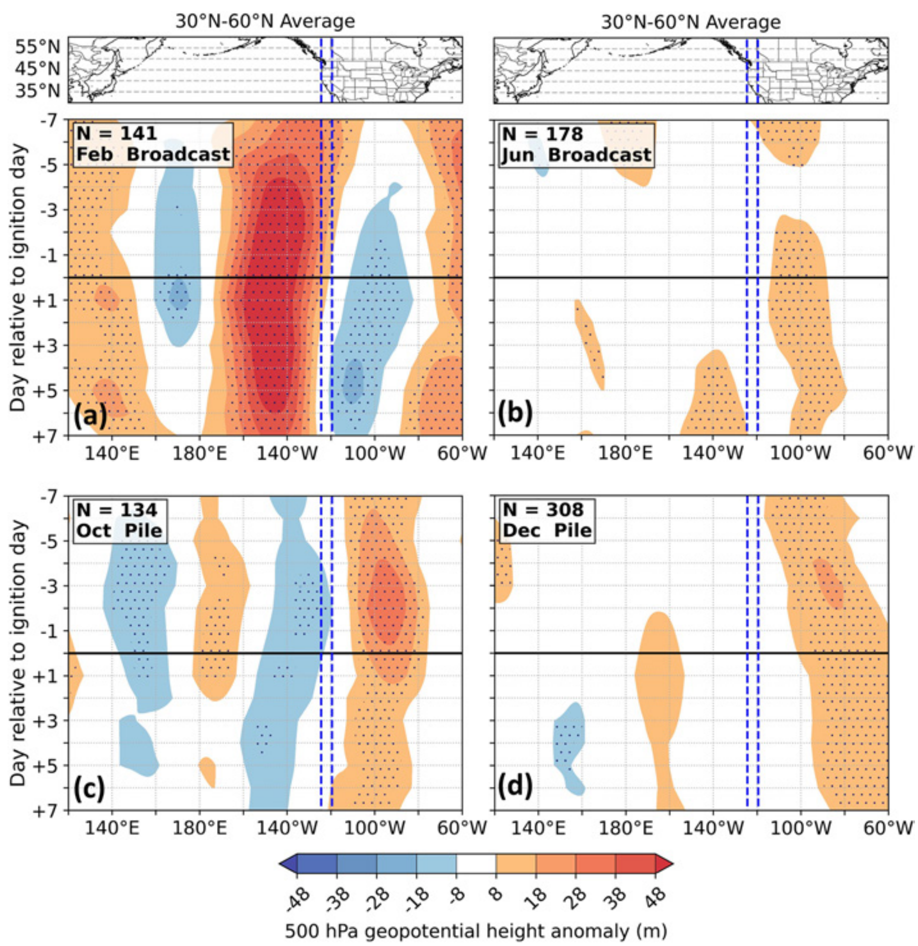


**Fig. 10** Hovmöller diagrams of composites of daily z500 anomalies associated with past **a**,**b** broadcast burns and **c**,**d** pile burns that occurred in ONCC from 2011 to 2024 organized by month: **a** February, **b** June, **c** October, and **d** December. Composite values at each longitude (horizontal axes) in Fig. 9 were averaged over the latitudinal band between 30° and 60° N depicted as the vertical area in the top subplots. Results are shown for each of the ± 7 days (vertical axes) relative to the ignition day (black, horizontal line). The blue, vertical lines indicate the longitudinal bounds of ONCC within the diagram. Stippling indicates that the anomaly is unlikely to have occurred by random chance at the 5% significance level using 10,000 bootstrapped samples with replacement. Figures for remaining months are in Additional file 4

agreement about the anomaly sign among the composite samples (59–41% split of positive and negative anomalies over ONCC, respectively; not shown). Slightly positive anomalies are observed east of ONCC in the week ahead and for several days after ignition of broadcast burns in June; otherwise, there is no systematic preference in the signal in the 2 weeks surrounding ignition day (Fig. 10b).

#### *Anomalous conditions before, during, and after past pile burns*

Figure 9c and d show the average of the daily z500 anomalies associated with past pile ignition days in October and December, respectively. October is selected because the local composites in Fig. 8 showed stronger anomalies for this month. December is selected because it is the most popular month (by count) for pile burning in our PFIRS subset.

October results show a narrow area of cyclonic (negative) anomalies over the northeastern Pacific Ocean and ONCC in an elongated west-east direction. 65% of the samples in the October pile composite have a negative anomaly over ONCC (not shown), indicating a consistent preference for anomalous troughing upstream and over ONCC on the day of ignition. Such large-scale troughing patterns are typically associated with lower surface temperatures, higher humidities, increased cloud cover and potentially precipitation. These conditions are consistent with those shown in the local composites for October pile burns (Fig. 8). Additionally, a sweeping, strong positive anomaly exists to the north expanding from the Aleutian Islands, Alaska to the southcentral US. This longitudinal-varying pattern of positive and negative anomalies in Fig. 9c persists in the 2 weeks centered on past October pile ignition days, as seen in the Hovmöller diagram in Fig. 10c. We see that a negative anomaly approaches closer to ONCC (blue, dashed lines) in the 4 days prior to ignition day. It then retreats westward as an anomalous ridge builds in the area within 6 days of ignition. This evolution indicates a short window of time to conduct pile burns under cooler and moister conditions.

December does not show a positive or negative composite anomaly near ONCC (Fig. 9d). The December pile composite had considerable disagreement among the composite samples about the sign of the anomaly near ONCC; 55% (45%) of the samples have a negative (positive) anomaly (not shown). This result indicates that there is less preference for a specific synoptic condition in order to conduct pile burns in December; a wide range of conditions are used for pile burns this month. As such, the Hovmöller diagram (Fig. 10d) shows that there is no pattern within the composite anomaly over ONCC in the 2 weeks surrounding ignition day. However, there is an eastward propagating signal of weak positive anomalies just to the east of ONCC indicating that anomalous ridging is typically present over the western and central US the week before ignition.

### Average monthly occurrence of burn windows

We determined the average number of burn windows during 2005–2024 for each month and each gridMET grid cell in ONCC according to the steps described in the third subsection of the Methods. We focus results on February and October, because these months have a relatively high number of burn days for one burn type while exhibiting relatively few burn days for the other type.

#### *Average number of burn days in February*

The average number of potential burn days in February is much greater for pile than for broadcast burns (top row of Fig. 11); GACC-wide, there are on average ~13 (46%) days of the month that meet criteria for pile burning while only ~7 (24%) days meet broadcast-burn criteria. The greatest number of opportunities (>10 days) for broadcast burning are concentrated in the Foothills, the lower-elevation areas of the Klamath, and the Coast ecoregions (Fig. 11a). The majority of ONCC has >10 potential pile burn days in February; however, the greatest opportunity (>15 days) occurs in the southern portions of the Valley, Foothills, and Sierra ecoregions and large swaths of the Northeast ecoregion (Fig. 11c).

Reasons for the relatively low number of broadcast burn windows across ONCC compared to the number of pile burn windows are revealed in postage-stamp maps of the different variables comprising the conditions criteria (Fig. 12). These maps show the average number of days in February that fall outside of criteria as a result of the variable either being below or above the criteria range. As such, regions with high counts in Fig. 12 coincide with regions with relatively low burn opportunities in Fig. 11 (top row). We see that max-t, avg-DFM100hr, avg-DFM1000hr are the most limiting variables to meeting typical broadcast burn conditions in February (larger counts in Fig. 12a). These variable limitations are mostly one-sided, meaning that the largest counts of falling outside of criteria are because max-t was too low and avg-DFM100hr and avg-DFM1000hr were too high (i.e., conditions were too cool or moist). There are few instances where criteria are missed because max-t is too high or the fuel moisture is too low to conduct a broadcast burn this time of year. Avg-wspd and max-vi put conditions out of criteria because they are either too low or too high, while avg-BI and ndays_since_wp are almost never limiting factors for broadcast burns in February. Compared to broadcast burns, fewer limitations appear for pile burning (Fig. 12b), resulting in higher burn opportunity counts (Fig. 11c).

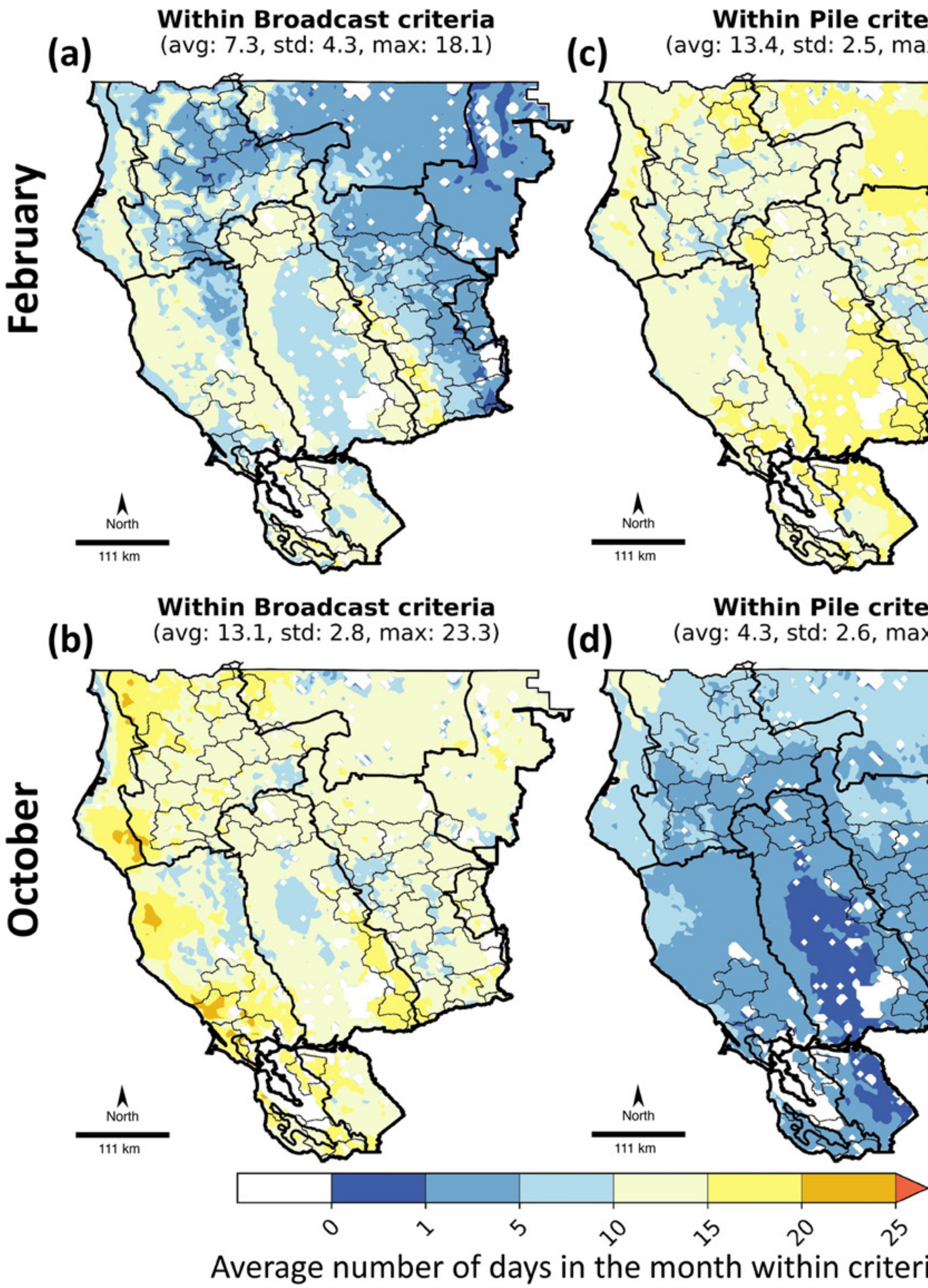


**Fig. 11** Average (mean) number of top) February and bottom) October days from 2005–2024 that fell within typical **a**,**b** broadcast and **c**,**d** pile burn-day conditions. Conditions criteria are based on processes described in the third subsection of the Methods. Grid cells without defined criteria (< 10 samples) are masked with white. To aid in decision-making, we overlaid National Interagency Coordination Center predictive service areas (thick, black polygons) and high-risk firesheds (Evers et al. 2025; thin, black polygons). Numbers above the subplots indicate the GACC-wide average (avg), standard deviation (std), and maximum (max) of the number of burn days. Figures for remaining months are in Additional file 5

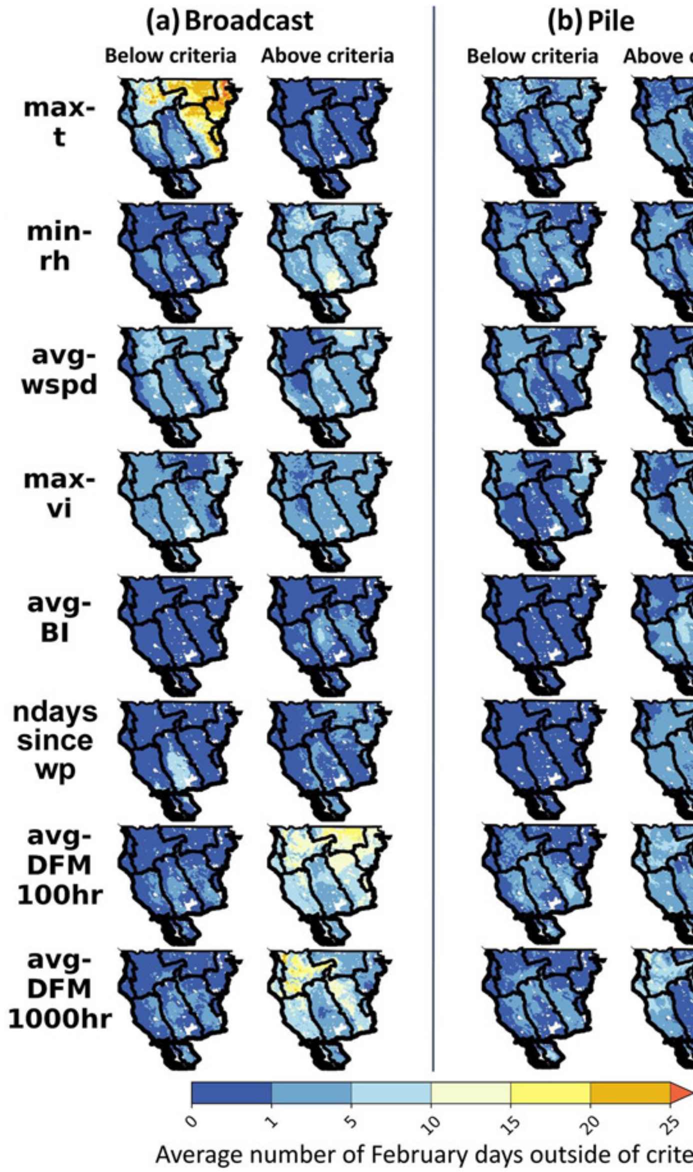


**Fig. 12** Average (mean) number of February days from 2005–2024 that fell outside of typical **a** broadcast and **b** pile burn-day conditions as a result of variables (rows) that were either below (left columns) or above (right columns) conditions criteria. Conditions criteria are based on processes described in the third subsection of the Methods. Grid cells without defined criteria (< 10 samples) are masked with white. National Interagency Coordination Center predictive service areas are outlined with black polygons. Figures for the remaining months are in Additional file 6

### *Average number of burn days in October*

There are more broadcast than pile burn opportunities in October (Fig. 11, bottom row). GACC-wide, there are on average ~13 (42%) days of the month that fall within the conditions criteria for broadcast burns, while only ~4 (13%) days meet pile burn conditions. The majority of ONCC meets broadcast conditions >10 days out of the month, with the greatest number of opportunities along the coastline and small sections of the Klamath and Foothills ecoregions. Pile burn opportunities are greatest (>5 days) in the northern tier of ONCC and parts of the central coastline.

Days fall outside of October broadcast burn conditions because most variables are either too low or too high (i.e., two-sided limitations), but the number of times that this occurs is relatively low (see Additional file 6). In contrast, for pile burning, conditions are often (10–25 days of the month, depending on the location) too warm, the atmosphere and fuels are too dry, the BI is too high, and it has been too long since the last wetting precipitation to safely conduct pile burns in October, especially in the Valley ecoregion and Diablo Range (Additional file 6).

## Discussion

### Considerations beyond the weather

By focusing our analysis on past go-burn days, we capture more nuance than just theoretically burnable conditions from a prescription perspective: we capture burn-practitioner preferences over 15,468 burns. This is most evident in the difference in the number of burn windows between the two burn types in a given month. In October, we saw approximately a third fewer pile than broadcast burn windows, because conditions were often too warm and dry to satisfy the typical conditions that practitioners conducted pile burns under (bottom row of Fig. 11 and Additional file 6). Given that environmental conditions were conducive to burning in general in October (as evidenced by the abundance of broadcast burn windows), the sparsity of pile burn windows must indicate external considerations beyond the presence of a "good fire environment." Even though consolidated, dry fuels within piles burn more intensely and with longer flame lengths than broadcast burns (California State Parks 2025), the projects are smaller and typically less complex in nature. This often means that fewer personnel and contingency resources are available to suppress any spot fires or undesired creeping fire behavior. These factors likely contribute to our findings that pile practitioners prefer a cooler and wetter environment in October–one that can help them achieve their objectives safely. Specifically, the median number of days since wetting precipitation across all vegetation-elevation subgroups (gray boxplots in Fig. 3 and Additional file 3) is only one day for pile and 10 days for broadcast burns in October. Additionally, the medians of the atmospheric and fuel moisture variables (avg-DFM100hr, avg-DFM1000hr, and min-rh) are also higher on pile burn days (18%, 17%, 49%) than on broadcast burn days (11%, 13%, 24%). This general shift in preference towards a recent wetting event and moister conditions for pile burns holds true for all months. Conducting pile burns during these moist conditions may allow for follow-up broadcast burn treatments once heavier fuel loads are removed from the area.

Conversely, we saw twice as many pile than broadcast burn windows in February (top row of Fig. 11). It is more feasible for practitioners to apply interventions (e.g., covering piles with paper or tarps to keep fuels dry or using leaf blowers for additional oxygen) to help piles burn. These interventions effectively "detach" pile burn requirements from current conditions by allowing pile practitioners to burn in an otherwise unfavorable, "too moist" fire environment. It should not be understated that the burn type and the objectives of the burn matter when assessing burn windows, because different burn types and objectives require different implementation strategies.

### Management implications

Our documentation of the location and timing of past prescribed burns and their corresponding environmental conditions can support adaptive management and decision making in several ways. Land and air-quality managers at the state and local levels can use this information to estimate times of year when burn permit requests and thus total smoke production (and resource requirements) might peak for different ecoregions at different elevations. For example, we saw evidence (Fig. 5a) of the use of broadcast burns to treat as much area as possible in June. Figure 6e showed that June burning is predominately split between crop broadcast burns in the Valley ecoregion and GSS in the Foothills ecoregion. Cropland burning in the Valley can result in high concentrations of air pollution from vertically trapped smoke that pools and stagnates in the regional topographic depression that forms the Sacramento Valley. This impacts visibility on roadways and public health (Bahardar 1993) and can limit approved burn permits in other areas in order to maintain Federal and State air-quality standards. While crop burning may be constrained around harvest time, or in viticultural areas, the period spanning fruit set, grape-ripening onset, and harvest of wine grapes, smoke managers, and land owners may be able to advocate for more burning of GSS in the Foothills in May instead of June. This would help to ensure that total smoke production remains below exceedance thresholds in June while also maximizing approvals for widespread prescribed burn permits before the peak fire season begins. There are overall more broadcast and pile burn windows in May than in June, including in the high-risk firesheds (see Additional file 7), supporting this shift.

Burn bosses and fire meteorologists could use numerical weather prediction forecast models to identify similar z500 anomaly patterns (see fourth subsection of the Results) in order to anticipate burn windows, hours-to-weeks in the future. Publicly available access to these forecasts from a variety of short- and long-range forecast models are available from graphical forecast websites linked in the Availability of data and materials section. We caution that forecast skill tends to degrade with lead time (Slingo and Palmer 2011; Worsnop et al. 2021), and that composite conditions are not the only setups that are conducive to prescribed burning. Future work will explore the variability in the daily z500 patterns that make up the monthly composites. Knowledge of burn seasonality and the common patterns for burning as shown can also provide additional lead time for community-awareness campaigns. These campaigns prepare the public for upcoming periods where smoke impacts may occur and provide training on protective actions during active burn periods to mitigate negative effects from smoke on health and local economies.

From a weather perspective, our analysis indicates potential to scale up prescribed burning. Our approach provided conservative estimates of burn windows, in which conditions on a given day and location must have simultaneously fallen within all of the variables' 5th and 95th percentiles (see third subsection of the Methods). Even then, we found that each month had locations across ONCC with 15 or more available burn days (Fig. 11 and Additional file 5). Figures in Additional file 2 illustrate burn windows based on minima-maxima criteria (0th and 100th percentiles; see third subsection of the Methods) and provide more of an upper bound for the number of burn windows. In this case, many locations have available burn windows for 25 or more days of the month, especially during October-May. Treatments can be maximized each month if burn projects target opportune areas where desired burn types can be safely and effectively implemented. We also illustrate this potential scalability in Fig. 13, which is a recreation of Fig. 5 using the theoretical number of burn windows that could have happened from 2011 to 2024 in ONCC by tabulating the number of grid cells that met our definition of typical burn conditions on any given day. While it is obviously implausible to burn such large portions of ONCC in a day, Fig. 13 illustrates (1) an abundant number of burn windows each year across much of ONCC and (2) that interannual variability of the conditions modifies the number of opportunities. It also highlights the number of potential days of "good fire weather" when positive effects from fire either from prescribed burns or wildfires managed for resource benefits can be realized (Hatchett and Wells 2026). Similar findings of interannual variability were found for burn windows in the southeastern US in association with phases of the El Niño-Southern Oscillation (Chiodi et al. 2018). Diagnosis of the causes of variability in ONCC, including linkages to large-scale climate patterns could provide further insight into the expected number of burn opportunities. Having flexible approval policies and developing community capacity will enable burn practitioners to seize opportunities in months with ample burn windows to help meet the goal of restoring pre-exclusion fire-return intervals.

### Limitations and future work

A key limitation of our analysis is that our daily, gridded reanalyses cannot fully capture observed conditions at the spatial scale of the many burns that are on the order of 1–1000 acres (recall one gridMET gridcell occupies nearly 4000 acres). Knowledge of localized and regional terrain-induced effects on wind, temperature, humidity, stability, and precipitation (Jiménez and Dudhia 2012; Stuart et al. 2025) may change the estimated number of burn days. In addition, the daily data cannot account for the fact that only several hours of in-prescription conditions may be needed to accomplish objectives; these estimates provide the bounds of the prescription at the daily scale but hourly assessments could further refine these bounds to cover the specific hours of active burning. Requiring ignition start and completion times as part of burn reporting would help studies further constrain these estimates. Even though our data show that past burns often happened on days with wetting precipitation (indicated by bottom whiskers in Fig. 3 and Additional file 3), it is plausible that burns were planned with precipitation expected after ignition to support unit securement. Future work is needed to quantify the relationship between the timing of prescribed burns and sub-daily precipitation to refine estimates of burn windows. Because no data were available on whether burn objectives were met, we could not quantify the conditions differentiating burns meeting versus not meeting objectives. Last, additional years of prescribed burns could provide a large enough dataset to estimate the number of burn windows on sub-monthly timescales and to explore if there are any agency-based differences in preferred conditions, which may reflect agency (or practitioner) priorities.

## Conclusions

Using 15,468 prescribed burn permits from 2011 to 2024, we identified strong seasonality in the timing and location of past broadcast and pile burns ignited in the Northern California Geographical Area Coordination Center region, and their associated local- and large-scale weather patterns. The recent acceleration in pile and broadcast burning and the implementation of the policies calling for additional burning (e.g., the USFS Wildfire Crisis Strategy) underscore the value and need for identification of burn windows of opportunity. We used a novel approach to define prescription criteria, separately for each burn type, for burn windows based on past "go-burn" days and provided monthly estimates of the location and frequency of occurrence of those windows, which can aid in project planning, resource allocation, and community outreach and engagement. From a weather perspective, we found ample burn windows across ONCC to support an increase in prescribed burning activity. Our methods could be refined to test the sensitivity of relaxing certain variables within our prescription criteria (Chiodi et al. 2019) in order to open up even more burn windows. Expanding this work elsewhere is possible if there are data detailing

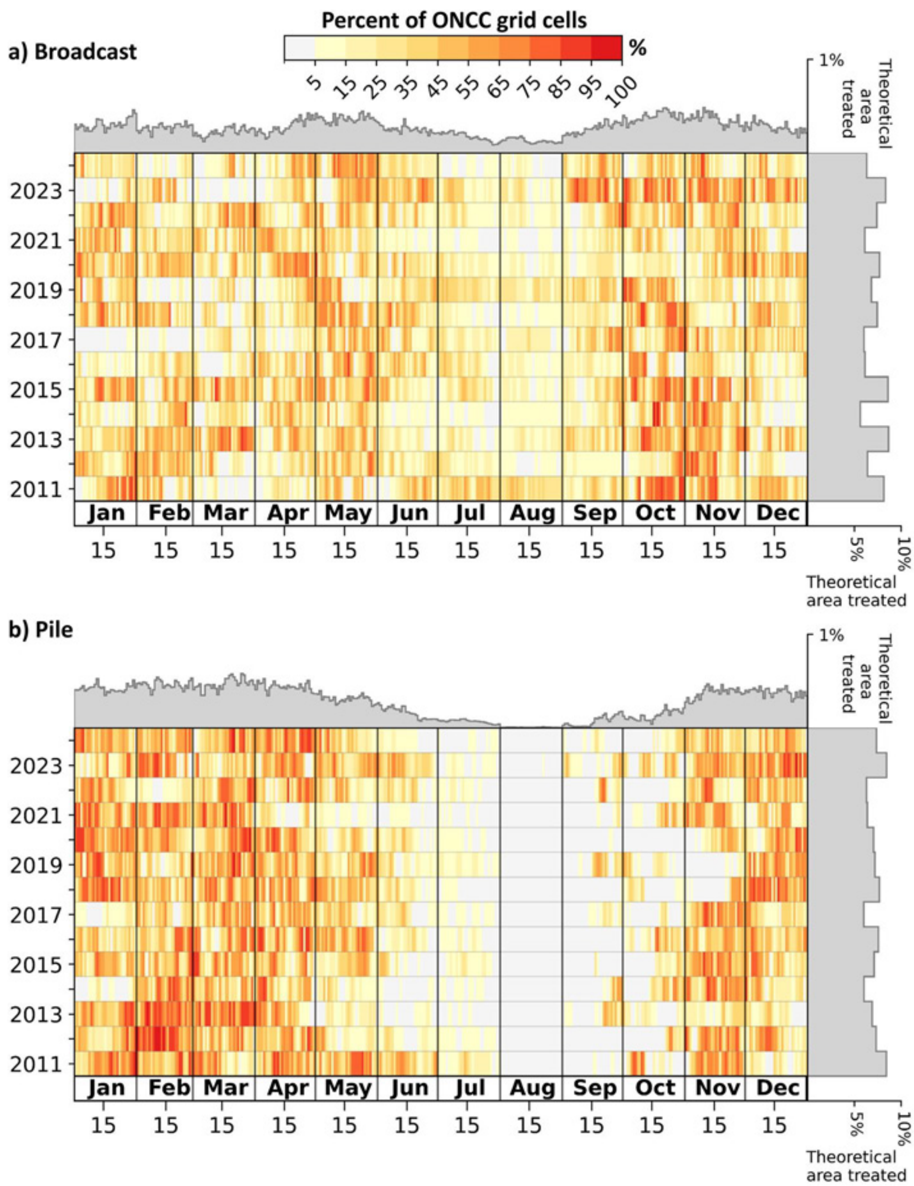


**Fig. 13** Amount of theoretical prescribed burns that could have occurred within ONCC on each day (horizontal axes) for each year (vertical axes) between 2011 and 2024, expressed as percent of total ONCC grid cells (yellow–red colorbar). Theoretical occurrence is based on whether conditions met typical conditions criteria described in the third subsection of the Methods. Red shades indicate a greater proportion of grid cells in ONCC that met typical burn conditions. Gray histograms on top of the subplots indicate the percent of the total theoretical area burned by the theoretical prescribed burns on any given day. Histograms on the right side of the subplots indicate the percent of the total theoretical area burned by theoretical prescribed burns each year. Area is determined by multiplying the area of the 4-km grid cell by the number of grid cells that met criteria. Broadcast burns are shown in **a** and pile burns in **b**

the day-of-ignition, location, and burn type. Future collection of information about the temporal progression of the burns (i.e., timing of test fire-ignitions to unit securement), associated observed weather and fuels conditions, the resultant fire and smoke behavior, and whether burn objectives were met would facilitate research into the range of conditions required to achieve success. The more-comprehensive data would also support further verification of long-lead (e.g., Worsnop et al. 2020, 2021; Breeden et al. 2025) and spot-weather forecasts used to support burning (e.g., Nauslar et al. 2016).

## Abbreviations

| | |
|---|---|
| AGL | Above ground level |
| ASL | Above sea level |
| BI | Burning Index of the NFDRS |
| EPA | US Environmental Protection Agency |

| | |
|---|---|
| GACC | Geographic Area Coordination Center |
| GSS | Grass, savanna, or shrub |
| IGBP | International Geosphere Biosphere Programme |
| MODIS | Moderate Resolution Imaging Spectroradiometer |
| NFDRS | US Forest Service National Fire Danger Rating System |
| NLDAS-2 | North American Land Data Assimilation System Phase 2 |
| NOAA | National Oceanic and Atmospheric Administration |
| ONCC | Northern California Geographic Area Coordination Center |
| PFIRS | Prescribed Fire Incident Reporting System |
| PRISM | Parameter-elevation Regressions on Independent Slopes Model |
| PSL | Physical Sciences Laboratory |
| SMP | Smoke management plan |
| US | United States of America |

## Supplementary Information

The online version contains supplementary material available at https://doi.org/10.1186/s42408-026-00492-6.

Additional file 1.
Additional file 2.
Additional file 3.
Additional file 4.
Additional file 5.
Additional file 6.
Additional file 7.

**Acknowledgements**
We gratefully acknowledge the anonymous reviewers and Dr. Erin Towler (NOAA/PSL) for feedback that helped improve this manuscript. We thank S. Li from University of California, Irvine for sharing their California escaped prescribed fire dataset, K. Blankenship from The Nature Conservancy for sharing PFIRS data, and J. Branz from California Air Resources Board for insightful discussions regarding California prescribed fire and smoke management operations.

**Authors' contributions**
RPW conceptualized the study, performed the analysis, visualization, and interpretation of results, and drafted the manuscript. TC collected and performed initial PFIRS data download and processing. All authors contributed to analysis ideas and provided editorial input throughout the project and during manuscript preparation. The authors read, provided reviews, and approved the final manuscript.

**Funding**
NOAA Physical Sciences Laboratory supported RPW's time during analysis and manuscript preparation. BJH was supported in part by the NOAA Cooperative Agreement NA19OAR4320073 for the Cooperative Institute for Research in the Atmosphere.

**Data availability**
The datasets analyzed or mentioned in the current study are available at the following hyperlinks and are referenced where they were first described.
PFIRS: https://ssl.arb.ca.gov/pfirs/ and via contact with Jason Branz at the California Air Resources Board
gridMET: https://www.climatologylab.org/gridmet.html
ERA5:
We used a combination of ERA5 data available in-house at NOAA/Physical Sciences Laboratory in Boulder, CO, US and from the websites below:
https://cds.climate.copernicus.eu/datasets/reanalysis-era5-single-levels?tab=downloadhttps://cds.climate.copernicus.eu/datasets/reanalysis-era5-pressure-levels?tab=download
EPA Level III ecoregions shapefiles:
https://www.epa.gov/eco-research/ecoregion-download-files-state-region-9#pane-04
MODIS MCD12C1 Version 6.1 IGBP land cover class product: https://appeears.earthdatacloud.nasa.gov/
GACC shapefiles:
https://data-nifc.opendata.arcgis.com/datasets/614ad98bdf834c92bf92c4f0fe197903_0/explore?location=1.387252%2C0.314277%2C1.65
National Interagency Coordination Center predictive service area shapefiles:
https://data-nifc.opendata.arcgis.com/datasets/45ff876436e34182aee63f3ac352fb8b_0/explore?location=31.492249%2C-98.681235%2C4.96
ArcGIS Fireshed Registry to isolate IDs associated with high-risk firesheds:
https://www.arcgis.com/home/item.html?id=3e38347fd53444c994fe4407e9206cd9#data
Graphical forecast websites for z500 anomalies:
Pivotal Weather: https://www.pivotalweather.com/model.php?rh=2025091600&fh=0&dpdt=&mc=&r=na&p=500h_anom-mean&m=gefsens
Tropical Tidbits: https://www.tropicaltidbits.com/analysis/models/?model=gfs-ens&region=namer&pkg=z500a&runtime=2025091612&fh=6

## Declarations

**Ethics approval and consent to participate**
Not applicable.

**Consent for publication**
Not applicable.

**Competing interests**
The authors declare no competing interests.

**Author details**
[1]NOAA/Physical Sciences Laboratory, 325 Broadway, Boulder, CO, USA. [2]Cooperative Institute for Research in the Atmosphere, Colorado State University, Fort Collins, CO, USA. [3]Affiliate working on a cooperative grant with the NOAA/Global Systems Laboratory, Boulder, CO, USA. [4]The Nature Conservancy, Arlington, VA 22203, USA. [5]NOAA/Global Systems Laboratory, Boulder, CO, USA. [6]USDA Forest Service, Rocky Mountain Research Station, Missoula Fire Sciences Laboratory, Missoula, MT 59808, USA. [7]Cooperative Institute for Research in Environmental Sciences, University of Colorado Boulder, Boulder, CO, USA.

Received: 30 December 2025 Accepted: 7 April 2026
Published online: 04 May 2026

**References**
Abatzoglou, John T. 2011. Development of gridded surface meteorological data for ecological applications and modelling. *International Journal of Climatology* 33 (1): 121–131. https://doi.org/10.1002/joc.3413.
Bahardar, M. B. 1993. *Rice field burning, policies and alternatives to burning, in the Sacramento Valley, producer's side*. PhD dissertation, University of California Davis. Accessed on 2026-FEB-23 from https://www.proquest.com/openview/03d923773f07bf12856128316f81409f/1?cbl=18750&diss=y&pq-origsite=gscholar.
Baijnath-Rodino, J. A., S. Li, A. Martinez, M. Kumar, L. N. Quinn-Davidson, R. A. York, and T. Banerjee. 2022. Historical seasonal changes in prescribed burn windows in California. *Science of the Total Environment* 836:155723. https://doi.org/10.1016/j.scitotenv.2022.155723.
Bradshaw, L. S., J. E. Deeming, R. E. Burgan, J. D. Cohen, and compilers. 1984. *The 1978 National Fire-Danger Rating System: Technical documentation*. Gen. Tech. Rep. INT-169, 44. Ogden, UT: USDA Forest Service, Intermountain Forest and Range Experiment Station, https://research.fs.usda.gov/treesearch/29615.
Breeden, M. L., A. Hoell, R. P. Worsnop, J. R. Albers, M. Hobbins, R. M. Robinson, and D. J. Vimont. 2025. Seasonal predictability of vapor pressure deficit in the western United States. *Weather and Climate Dynamics* 6 (4): 1443–1459. https://doi.org/10.5194/wcd-6-1443-2025.
California State Parks. 2025. *Frequently asked questions: How does State Parks decide when to conduct prescribed burns?* Accessed on 2025-AUG-01 from https://www.parks.ca.gov/?page_id=31646.
CARB, California Air Resources Board. 2026. *Agricultural burning*. Accessed on 2026-FEB-23 from https://ww2.arb.ca.gov/our-work/programs/agricultural-burning.

Carlson, J. D., L. S. Bradshaw, R. M. Nelson, R. R. Bensch, and R. Jabrzemski. 2007. Application of the Nelson model to four timelag fuel classes using Oklahoma field observations: Model evaluation and comparison with National Fire Danger Rating System algorithms. *International Journal of Wildland Fire* 16 (2): 204–216. https://doi.org/10.1071/wf06073.
Chiodi, A. M., N. S. Larkin, and J. M. Varner. 2018. An analysis of southeastern US prescribed burn weather windows: Seasonal variability and El Niño associations. *International Journal of Wildland Fire* 27:176–189. https://doi.org/10.1071/WF17132.
Chiodi, A. M., N. K. Larkin, J. M. Varner, and J. K. Heirs. 2019. Sensitivity of prescribed burn weather windows to atmospheric dispersion parameters over southeastern USA. *International Journal of Wildland Fire* 28:589–600. https://doi.org/10.1071/WF18209.
Daly, C., M. Halbleib, J. I. Smith, W. P. Gibson, M. K. Doggett, G. H. Taylor, J. Curtis, and P. P. Pasteris. 2008. Physiographically sensitive mapping of climatological temperature and precipitation across the conterminous United States. *International Journal of Climatology* 28 (15): 2031–2064. https://doi.org/10.1002/joc.1688.
Davis, K. T., J. Peeler, J. Fargione, R. D. Haugo, K. L. Metlen, M. D. Robles, and T. Woolley. 2024. Tamm review: A meta-analysis of thinning, prescribed fire, and wildfire effects on subsequent wildfire severity in conifer dominated forests of the Western US. *Forest Ecology and Management* 561:121885. https://doi.org/10.1016/j.foreco.2024.121885.
Deeming, J. E. 1972. *National Fire-Danger Rating System*. USDA Forest Service research paper RM-84. Fort Collins, CO: Rocky Mountain Forest and Range Experiment Station, https://doi.org/10.5962/bhl.title.98933.
Deeming, J. E., R. E. Burgan, and J. D. Cohen. 1977. *The National Fire-Danger Rating System–1978*. Revisions to the 1978 National Fire-Danger Rating System. Gen. Tech. Rep. INT-39, 63. Ogden, UT: USDA Forest Service, Intermountain Forest and Range Experiment Station, https://research.fs.usda.gov/treesearch/65268.
Efron, B. 1979. Bootstrap methods: Another look at the jackknife. *The Annals of Statistics* 7 (1): 1–26. https://doi.org/10.1214/aos/1176344552.
EPA. 2012. *US Environmental Protection Agency Level III ecoregions of California*. Distributed by US EPA Office of Research and Development (ORD) - National Health and Environmental Effects Research Laboratory (NHEERL), Corvallis, OR. ftp://ftp.epa.gov/wed/ecoregions/ca/ca_eco_l3.zip, http://edg.epa.gov.
Evers, C. R., C. D. Ringo, A. A. Ager, M. A. Day, A. Urdíroz, J. Fermin, and K. Bunzel. 2025. *The Fireshed Registry: Fireshed and subfireshed boundaries for the continental United States and Hawaii*. 4th Edition. Fort Collins, CO: USDA Forest Service Research Data Archive, https://doi.org/10.2737/RDS-2020-0054-4.
Fearon, M. G., T. J. Brown, and G. M. Curcio. 2015. Establishing a national standard method for operational mixing height determination. *Journal of Operational Meteorology* 3 (15): 172–189. http://dx.doi.org/10.15191/nwajom.2015.0315.
Fernandes, P. M., and H. S. Botelho. 2003. A review of prescribed burning effectiveness in fire hazard reduction. *International Journal of Wildland Fire* 12 (2): 117–128. https://doi.org/10.1071/wf02042.
Friedl, M., and D. Sulla-Menashe. 2022. *MODIS/Terra+Aqua land cover type yearly L3 global 500m SIN grid V061*. NASA Land Processes Distributed Active Archive Center. Accessed on 2025-SEP-26 from https://doi.org/10.5067/MODIS/MCD12Q1.061.
Hardy, C. C., R. D. Ottmar, J. L. Peterson, J. E. Core, and P. Seamon. 2001. *Smoke management guide for prescribed fire: 2001 edition*. National Wildfire Coordination Group, Tech. Rep. PMS 420–2, 236. Boise, ID, USA. https://www.fs.usda.gov/pnw/pubs/journals/pnw_2001_ottmar001.pdf.
Hatchett, B. J., and E. M. Wells. 2026. *Good fire weather*. Bulletin of the American Meteorological Society. BAMS-D-25-0209.1. https://doi.org/10.1175/BAMS-D-25-0209.1, in press.
Hersbach, H., B. Bell, P. Berrisford, Shoji Hirahara, András Horányi, Joaquín Muñoz-Sabater, Julien Nicolas, Carole Peubey, Raluca Radu, Dinand Schepers, Adrian Simmons, Cornel Soci, Saleh Abdalla, Xavier Abellan, Gianpaolo Balsamo, Peter Bechtold, Gionata Biavati, Jean Bidlot, Massimo Bonavita, Giovanna De Chiara, Per Dahlgren, Dick Dee, Michail Diamantakis, Rossana Dragani, Johannes Flemming, Richard Forbes, Manuel Fuentes, Alan Geer, Leo Haimberger, Sean Healy, Robin J.. Hogan, Elías. Hólm, Marta Janisková, Sarah Keeley, Patrick Laloyaux, Philippe Lopez, Cristina Lupu, Gabor Radnoti, Patricia de Rosnay, Iryna Rozum, Freja Vamborg, Sebastien Villaume, and Jean-Noël. Thépaut. 2020. The ERA5 global reanalysis. *Quarterly Journal of the Royal Meteorological Society* 146 (730): 1999–2049. https://doi.org/10.1002/qj.3803.
Hersbach, H., B. Bell, P. Berrisford, G. Biavati, A. Horányi, J. Muñoz Sabater, J. Nicolas, C. Peubey, R. Radu, I. Rozum, D. Schepers, A. Simmons, C. Soci, D. Dee, and J-N Thépaut. 2023a. *ERA5 hourly data on single levels from 1940 to present*. Copernicus Climate Change Service (C3S) Climate Data Store (CDS), Accessed on 2024-DEC-08 from https://doi.org/10.24381/cds.adbb2d47.
Hersbach, H., B. Bell, P. Berrisford, G. Biavati, A. Horányi, J. Muñoz Sabater, J. Nicolas, C. Peubey, R. Radu, I. Rozum, D. Schepers, A. Simmons, C. Soci, D. Dee, and J-N Thépaut. 2023b. *ERA5 hourly data on pressure levels from 1940 to present*. Copernicus Climate Change Service (C3S) Climate Data Store (CDS), Accessed on 2024-DEC-08 from https://doi.org/10.24381/cds.bd0915c6.
Hiers, J. K., J. J. O'Brien, J. M. Varner, B. W. Butler, M. Dickinson, J. Furman, M. Gallagher, D. Godwin, S. L. Goodrick, S. M. Hood, A. Hudak, L. N. Kobziar, R. Linn, E. L. Loudermilk, S. McCaffrey, K. Robertson, E. M. Rowell, N. Skowronski, A. C. Watts, and K. M. Yedinak. 2020. Prescribed fire science: The case for a refined research agenda. *Fire Ecology* 16 (1) : 11. https://doi.org/10.1186/s42408-020-0070-8.
Holden, Z. A., A. Swanson, C. H. Luce, W. M. Jolly, M. Maneta, J. W. Oyler, D. A. Warren, R. Parsons, and D. Affleck. 2018. Decreasing fire season precipitation increased recent western US forest wildfire activity. *Proceedings of the National Academy of Sciences* 115 (36): E8349–E8357.
Hopkinson, P., M. Hammond, J. W. Bartolome, and L. Macaulay. 2020. Using consecutive prescribed fires to reduce shrub encroachment in grassland by increasing shrub mortality. *Restoration Ecology* 28:850–858. https://doi.org/10.1111/rec.13138.
Jiménez, P. A., and J. Dudhia. 2012. Improving the representation of resolved and unresolved topographic effects on surface wind in the WRF model. *Journal of Applied Meteorology and Climatology* 51 (2): 300–316. https://doi.org/10.1175/JAMC-D-11-084.1.
Jolly, W. M., P. H. Freeborn, L. S. Bradshaw, J. Wallace, and S. Brittain. 2024. Modernizing the US National Fire Danger Rating System (version 4): Simplified fuel models and improved live and dead fuel moisture calculations. *Environmental Modelling & Software* 181:106181. https://doi.org/10.1016/j.envsoft.2024.106181.
Keeley, J. E., R. C. Klinger, T. J. Brennan, D. M. Lawson, J. La Grange, and K. N. Berg. 2023. A decade-long study of repeated prescription burning in California native grassland restoration. *Restoration Ecology* 31:e13939. https://doi.org/10.1111/rec.13939.
Kjaer, E. L., R. Limb, B. Geaumont, J. Harmon, T. Hovick, and K. Sedivec. 2025. Fire and grazing reduce invasive grass thatch in rangelands. *Rangeland Ecology and Management* 98:414–418. https://doi.org/10.1016/j.rama.2024.06.009.
Knapp, E. E., J. M. Lydersen, M. P. North, and B. M. Collins. 2017. Efficacy of variable density thinning and prescribed fire for restoring forest heterogeneity to mixed-conifer forest in the central Sierra Nevada, CA. *Forest Ecology and Management* 406:228–241. https://doi.org/10.1016/j.foreco.2017.08.028.
Li, S., J. A. Baijnath-Rodino, R. A. York, L. N. Quinn-Davidson, and T. Banerjee. 2025. Temporal and spatial pattern analysis of escaped prescribed fires in California from 1991 to 2020. *Fire Ecology* 21 (1). https://doi.org/10.1186/s42408-024-00342-3.
Miller, R. K., C. B. Field, and K. J. Mach. 2020. Barriers and enablers for prescribed burns for wildfire management in California. *Nature Sustainability* 3 (2): 101–109. https://doi.org/10.1038/s41893-019-0451-7.
Mitchell, K. E., D. Lohmann, P. R. Houser, E. F. Wood, J. C. Schaake, A. Robock, B. A. Cosgrove, J. Sheffield, Q. Duan, L. Luo, R. W. Higgins, R. T. Pinker, J. D. Tarpley, D. P. Lettenmaier, C. H. Marshall, J. K. Entin, M. Pan, W. Shi, V. Koren, J. Meng, B. H. Ramsay, and A. A. Bailey. 2004. The multi-institution North American Land Data Assimilation System (NLDAS): Utilizing multiple GCIP products and partners in a continental distributed hydrological modeling system. *Journal of Geophysical Research: Atmospheres* 109 (D7). https://doi.org/10.1029/2003JD003823.
Nauslar, N. J., T. J. Brown, and J. D. Horel. 2016. Verification of National Weather Service spot forecasts using atmospheric sounding observations. *Journal of Operational Meteorology* 4 (4): 46–57. https://doi.org/10.15191/nwajom.2016.0404.
Noda, S. J. 2025. *Restoring California coastal prairies with pile burns: Effective shrub removal requires successive management to prevent re-encroachment*.

Master's thesis, University of California Davis. Accessed on 2026–FEB-23 from https://search.proquest.com/openview/7c5c6d3e00863c807b2fd3ebbe8aeb8a/1?pq-origsite=gscholar&cbl=18750&diss=y.
NWCG, National Wildfire Coordinating Group Prescribed Fire Plan Template, PMS 484–1. 2018. Accessed on 2026-MAR-02 from https://www.fs.usda.gov/sites/default/files/2022-07/Burn%20Plan.pdf.
Persson, A. 2017. The story of the Hovmöller diagram: An (almost) eyewitness account. *Bulletin of the American Meteorological Society* 98:949–957. https://doi.org/10.1175/BAMS-D-15-00234.1.
Quinn-Davidson, L. N., and J. M. Varner. 2012. Impediments to prescribed fire across agency, landscape and manager: An example from northern California. *International Journal of Wildland Fire* 21 (3): 210–218. https://doi.org/10.1071/wf11017.
Ryan, K. C., E. E. Knapp, and J. M. Varner. 2013. Prescribed fire in North American forests and woodlands: History, current practice, and challenges. *Frontiers in Ecology and the Environment* 11 (s1): e15–e24. https://doi.org/10.1890/120329.
Slingo, J., and T. Palmer. 2011. Uncertainty in weather and climate prediction. *Philosophical Transactions of the Royal Society a: Mathematical, Physical and Engineering Sciences* 369 (1956). https://doi.org/10.1098/rsta.2011.0161.
Stuart, S. J., S. M. Dean, A. N. Mackintosh, A. Sood, P. B. Gibson, S. Moore, and E. J. Kendon. 2025. Precipitation over complex mountain terrain in a convection-permitting regional climate model. *Journal of Geophysical Research: Atmospheres* 130 (12) : e2024JD042773. https://doi.org/10.1029/2024JD042773.
Swain, D. L., J. T. Abatzoglou, C. Kolden, K. Shive, D. A. Kalashnikov, D. Singh, and E. Smith. 2023. Climate change is narrowing and shifting prescribed fire windows in western United States. *Communications Earth & Environment* 4 (1). https://doi.org/10.1038/s43247-023-00993-1.
Title 17 of the Barclays California Code of Regulations. 2001. *Subchapter 2. Smoke management guidelines for agricultural and prescribed burning*. 26. Accessed on 2025-DEC-01 from https://ww2.arb.ca.gov/sites/default/files/2021-06/Title17.pdf.
Toman, E. M., B. Stidham, B. Shindler, and S. McCaffrey. 2011. Reducing fuels in the wildland–urban interface: Community perceptions of agency fuels treatments. *International Journal of Wildland Fire* 20 (3): 340–349. https://doi.org/10.1071/wf10042.
USFS. 2022. *Confronting the wildfire crisis: A 10-year implementation plan*. USDA Forest Service, Tech. Rep. FS-1187b, 11. https://www.fs.usda.gov/sites/default/files/Wildfire-Crisis-Implementation-Plan.pdf.
Vaillant, N. M., J. A. Fites-Kaufman, and S. L. Stephens. 2009. Effectiveness of prescribed fire as a fuel treatment in Californian coniferous forests. *International Journal of Wildland Fire* 18:165–175. https://doi.org/10.1071/WF06065.
Wade, D. D., and J. D., Lunsford. 1989. *A guide for prescribed fire in southern forests.* Tech. Rep. R8-TP 11, 63. USDA Forest Service Southern Region. https://www.landcan.org/pdfs/guide_for_prescribed_fire.pdf.
Weir, J. R. 2011. Are weather and tradition reducing our ability to conduct prescribed burns? *Rangelands* 33 (1): 25–30. https://doi.org/10.2111/RANGELANDS-D-10-00050.1.
Wilks, D. S. 2011. *Statistical methods in the atmospheric sciences*. 3rd ed. Amsterdam, The Netherlands: Elsevier Inc.
Worsnop, R. P., M. Scheuerer, and T. M. Hamill. 2020. Extended-range probabilistic fire weather forecasting based on ensemble model output statistics and ensemble copula coupling. *Monthly Weather Review* 148:499–521. https://doi.org/10.1175/MWR-D-19-0217.1.
Worsnop, R. P., M. Scheuerer, F. Di Giuseppe, C. Barnard, T. M. Hamill, and C. Vitolo. 2021. Probabilistic fire danger forecasting: A framework for week-two forecasts using statistical postprocessing techniques and the global ECMWF Fire Forecast System (GEFF). *Weather and Forecasting* 36 (6). https://doi.org/10.1175/WAF-D-21-0075.1.
Yurkonis, K. A., J. Dillon, D. A. McGranahan, D. Toledo, and B. J. Goodwin. 2019. Seasonality of prescribed fire weather windows and predicted fire behavior in the northern Great Plains, USA. *Fire Ecology* 15:7. https://doi.org/10.1186/s42408-019-0027-y.
Zamora-Reyes, D., B. Black, and V. Trouet. 2022. Enhanced winter, spring, and summer hydroclimate variability across California from 1940 to 2019. *International Journal of Climatology* 42 (9): 4940–4952. https://doi.org/10.1002/joc.7513.

## Publisher's Note